LAUNCH VEHICLE WIND RESPONSE

BY STATISTICAL METHODS

HAYES

INTERNATIONAL CORPORATION

BIRMINGHAM, ALABAMA

HAYES INTERNATIONAL CORPORATION
Birmingham, Alabama

LAUNCH VEHICLE WIND RESPONSE BY STATISTICAL METHODS

ENGINEERING REPORT
NO. 1193

29 November 1965

PREPARED BY:

J. E. Bailey

APPROVED BY:

Harry Passmore, III
Project Engineer

C. L. Anker
Project Manager

P. R. Coulson
Program Manager

REVISIONS

DATE	PAGES AFFECTED	REMARKS	BY	APP.

FORM E-509 REV. 2/3/61

ABSTRACT

24547

A new approach to the problem of large flexible booster response to lateral wind inputs during launch is used as a means of simplifying the load minimum control problem. Statistical analysis methods, which include generalized harmonic analysis and adjoint techniques are used to provide a different approach to the control law evaluation and optimization procedure.

Statistical techniques applicable to the problem of launch vehicle response calculation are discussed for the general case which includes a time varying system mathematical model and nonstationary random input process. The input process (i.e. the lateral wind input) is assumed to be stationary in space and time varying due only to the changing vehicle velocity. Methods are presented for determining root-mean-square bending moment and lateral drift for stationary constant coefficient system models and the general nonstationary case.

Various representations of the wind input are presented and their degree of simulation of the general wind profile data is discussed.

Finally, as a means of illustrating application of the techniques which are previously discussed, a constant coefficient Saturn V model at maximum dynamic pressure is studied. Effect of various control system feedback schemes on load and drift are presented.

Mr. R. S. Ryan, Chief, Dynamic Analysis Branch of the Flight Mechanics and Dynamics Division of the Aero-Astrodynamics Laboratory was the technical supervisor and the work reported herein was accomplished under contract NAS8-20201 with Marshall Space Flight Center National Aeronautics and Space Administration.

Author

TABLE OF CONTENTS

TITLE	PAGE
LIST OF FIGURES	i
LIST OF SYMBOLS	iv
INTRODUCTION	1
APPLICATION OF STATISTICAL THEORY TO FLEXIBLE BOOSTER RESPONSE	3
TIME-INVARIANT SYSTEM RESPONSE TO A STATIONARY PROCESS	9
DEFINITION OF THE WIND INPUT SPECTRA	18
APPLICATION TO A SATURN V MODEL	22
CONCLUSIONS AND RECOMMENDATIONS	26
REFERENCES	28
APPENDIX A - ANALOG SIMULATION	45

LIST OF FIGURES

FIGURE	TITLE	PAGE
1	DIRECT ANALOG DIAGRAM	30
2	ADJOINT ANALOG DIAGRAM	31
3	TYPICAL POWER SPECTRA OF ATMOSPHERIC TURBULENCE	32
4	WEIGHTING FILTER RESPONSE TO A UNIT IMPULSE	33
5	TYPICAL SYSTEM-WEIGHTING FUNCTION RESPONSE TO A 10 x UNIT IMPULSE	34
6	BENDING MOMENT WEIGHTING FUNCTIONS - EFFECT OF VARIATION IN ACCELEROMETER GAIN g_2	35
7	LATERAL DRIFT WEIGHTING FUNCTIONS - EFFECT OF VARIATION IN ACCELEROMETER GAIN g_2	36
8	EFFECT OF TURBULENCE SCALE FACTOR L ON SYSTEM WEIGHTING FUNCTION - L = 304	37
9	EFFECT OF TURBULENCE SCALE FACTOR L ON SYSTEM WEIGHTING - L = 1000	38
10	EFFECT OF ACCELEROMETER FEEDBACK ON LOAD RELIEF	39
11	EFFECT OF ACCELEROMETER FEEDBACK ON LATERAL DRIFT	40
12	EFFECT OF ACCELEROMETER GAIN ON 3σ BENDING MOMENT	41
13	EFFECT OF ANGLE OF ATTACK FEEDBACK ON 3σ BENDING MOMENT AND LATERAL DRIFT	42
14	EFFECT OF ANGLE OF ATTACK AND LATERAL DRIFT FEEDBACK ON 3σ LATERAL DRIFT AND BENDING MOMENT	43

LIST OF FIGURES

CONTINUED

FIGURE	TITLE	PAGE
15	EFFECT OF ACCELEROMETER GAIN g_2 ON 3σ BENDING MOMENT AND 3σ LATERAL DRIFT EFFECT OF L	44
16	ANALOG DIAGRAM	50

LIST OF SYMBOLS

a_o	Attitude loop gain of attitude control system
a_1	Rate loop gain of attitude control system
A_i	Indicated lateral acceleration
B_E	Elastic bending moment
BM	Total bending moment
B_R	Rigid body bending moment
D_1, D_2	Flexible vehicle aerodynamic coefficients
F_o, F_1	Rigid Vehicle aerodynamic coefficients
F-X	Thrust
F_s	Swivel engine thrust
g	Longitudinal acceleration of the vehicle
g_{2i}	Gain of accelerometer control loop
i	The number of accelerometers
I	Effective moment of inertia of the vehicle about its c. g.
j	The number of bending modes
m	Vehicle mass
m_1, m_2	Dynamic characteristics of engine gimbal system
M_{Bj}	Generalized bending mass
M'_α	Bending moment coefficient
M'_β	Bending moment coefficient for engine deflection

LIST OF SYMBOLS (CONTINUED)

Q	Dynamic pressure
t	Time
V	Vehicle Velocity
V_w	Lateral wind velocity
X_E	Coordinate of gimbal point (measured positive from center of gravity towards the tail of the vehicle)
X_{a_i}	Accelerometer location
X_K	Station for which bending moment is determined
Y	Translation displacement of rigid vehicle
Y_{ja_i}'	Displacement of bending mode at X_{a_i}
Y'_{ja_i}	Slope of bending mode at X_{a_i}
Y_{jE}'	Displacement of bending mode at X_E
Y'_{jE}	Slope of bending mode at X_E
Y'_{jg}	Slope of bending mode at position gyro location
α	Rigid body angle of attack
β	Swivel angle (angle of the engine gimbal relative to the center line of the vehicle at the gimbal point)
ζ_{a_i}	Damping factor of accelerometer
ζ_{Bj}	Damping factor of bending mode
η_j	Generalized bending coordinate
ϕ	Pitch angle of rigid vehicle relative to inertial space
ϕ_i	Indicated angle of rotation

LIST OF SYMBOLS (CONTINUED)

ω_{a_i}	Accelerometer frequency (rad/sec)
ω_{Bj}	Bending frequency (rad/sec)
$< >$	Denotes time average
$W_i(t, \tau)$	System weighting function
$F(t)$	System input
$\dot{Y}$	Lateral drift velocity
ϕ_{yy}	System output correlation function
$\phi_{v_w v_w}$	System input correlation function
$<Y^2(t)>$	Mean squared system output
α_G	Angle of attack due to a gust input
$\overline{Y}_1(t)$	White noise input process
$W^*(t, \tau)$	Combined system weighting function
$\delta(\tau)$	Unit impulse at $t = 0$
G_{yy}	Output spectral density function
$Y(j\omega)$	System transfer function
$G_{xx}(w)$	Input spectral density function
σ	Standard deviation

INTRODUCTION

The primary purpose of this report is to discuss application of statistical methods for control system analysis to the Saturn V launch vehicle during its flight in the atmosphere. During the past 20 years application of statistical methods to control system design has advanced to a point where engineering use of these techniques is feasible and commonplace. The development of the theory of "Generalized Harmonic Analysis" by Professor Norbert Wiener, which related the statistical description of a random process to its spectrum, has been the key to rapid development of the statistical theory of communication (Reference 1, Lee).

Recent trends in launch vehicle design have emphasized minimum load and minimum drift control techniques and considerable effort has been spent in analyzing and developing control systems, which minimize vehicle bending moment and lateral drift, primarily with time domain analysis methods, and very complex time-varying and perhaps nonlinear mathematical models of the launch vehicle. The bulk of the launch vehicle control system analysis in the past have been time domain studies of the vehicle responses to deterministic atmospheric disturbances and maneuvering requirements. Reliance on the outputs of these complicated vehicle models for system design information has in some cases let the trees obscure the forest. Basic fundamentals of the load relief and minimum drift problem are hidden by the complexity of the model output and by virtue of the time domain nature of the information. Based on available time domain derived information in statistical and deterministic form, the system trade offs are not easy to rate and even if a valid rating system can be determined the magnitude of all necessary computation per control system configuration is great.

Application of proven statistical methods of analysis to this problem shows promise of simplifying to some degree the complex trade-offs which occur in the large flexible booster control system. The concept of time domain analysis with a statistically determined deterministic wind profile has proved to yield a safe system design and has in a sense de-emphasized the frequency domain-statistical and the adjoint-analog approaches. Both methods offer the advantage of simplifying system analysis and yield a previously unobtainable picture of the system.

The function this report will serve is to review the powerful analytical methods which have, to a large extent, not been applied to the large flexible booster problem, and illustrate application of these techniques to problems currently of interest.

APPLICATION OF STATISTICAL THEORY TO FLEXIBLE BOOSTER RESPONSE

Determination of bending moment and lateral drift for large flexible launch vehicles with the aid of statistical methods is discussed in this section. The system mathematical model chosen for use in this analysis represents a Saturn V launch vehicle and simulates the following characteristics: (1) Rigid body rotational and translational degrees of freedom, (2) One bending mode, (3) Gimbal dynamics, (4) Feedback accelerometer dynamics, (5) Rigid body bending moment computation, (6) Linear aerodynamics.

The Laplace transformed system equations are presented in matrix notation as Equation 1 on the following page.

This set of linear equations describe the vehicle response to a lateral wind input and will be considered in general to have time varying coefficients because of varying vehicle velocity, air density, vehicle physical parameters, control system gains, etc. In matrix notation the vehicle equations become

$$\left[\, A \,\right] \left\{ Y \right\} = \left\{ B \right\} \left[\, V_w \,\right] \tag{2}$$

The solution of this set of linear equations with time varying coefficients may be expressed as

$$Y_i\,(t) = \int_{-\infty}^{t} W_i\,(t, \tau)\; F(\tau) d\tau \qquad i = 1,\ 2,\ 3,\ \ldots n \tag{3}$$

where $W_i(t, \tau)$ is defined as the general weighting function for the system of equations and is defined as the i-th output at time t obtained in the system response to a unit impulse applied at time τ, with all other inputs identically equal zero. $F\,(\tau)$ is the system input. Using this notation the bending moment response,

$$
\begin{bmatrix}
S^2 & 0 & -\frac{(F-X)}{I}(X_E Y'_{jE} - Y_{jE}) & \frac{F_s X_E}{I} & 0 & \frac{QF_1}{I} & 0 \\
\frac{F-X}{m} & -S^2 & -\frac{(F-X)}{m} Y'_{jE} & \frac{F_s}{m} & 0 & \frac{QF_o}{m} & 0 \\
0 & 0 & S^2 + 2\zeta_{jB}\omega_{Bj} S + \omega^2_{Bj} & \frac{-F_s Y_{jE}}{M_{Bj}} & 0 & \frac{-QD_j}{M_{Bj}} & 0 \\
-(a_o + a_1)S & 0 & Y'_{jg}(a_o + a_1 S) & (m_2 S^2 + m_1 S + 1) & -g_{2i} & 0 & 0 \\
(\omega^2_{a_i} X_{a_i} S^2 + g) & -\omega_{a_i}^2 & -(Y_{ja_i} S^2 + gY_{ja_i})\omega^2_{a_i} & 0 & (S^2 + 2\,{}_{a_i}\omega_{a_i} S + \omega_{a_i}^2) & 0 & 0 \\
-1 & \frac{S}{V} & 0 & 0 & 0 & 1 & 0 \\
0 & 0 & -M'_{\ddot{\eta}_j} S^2 & -M'_\beta & 0 & -M'_\alpha & 1
\end{bmatrix}
\begin{bmatrix}
\phi \\ Y \\ \eta_j \\ \beta \\ A_i \\ \zeta \\ B_{M_J}
\end{bmatrix}
=
\begin{bmatrix}
0 \\ 0 \\ 0 \\ 0 \\ 0 \\ \frac{1}{v} \\ 0
\end{bmatrix}
\begin{bmatrix} V_w \end{bmatrix}
$$

SYSTEM EQUATIONS

Equation 1

BM, and the lateral drift response, $\dot{Y}$, are

$$BM(t) = \int_{-\infty}^{t} W_{BM}(t, \tau)\, V_w(\tau)\, d\tau \tag{4}$$

$$\dot{Y}(t) = \int_{-\infty}^{t} W_{\dot{y}}(t, \tau)\, V_w(\tau) d\tau \tag{5}$$

System stability may be defined in terms of the weighting function and for a stable system

$$\int_{-\infty}^{\infty} \left| W(t, \tau) \right| d\tau < \text{constant} < \infty$$

Nonstationary System Response

For the case of a linear time variant system with a general random input, $v_w(t)$, that is stationary, the response Y(t) is from equation 3

$$Y_i(t) = \int_{-\infty}^{t} W_i(t, \tau_1) V_w(\tau)\, d\tau$$

To calculate the correlation function of the response we take

$$Y(t_1)\, Y(t_2) = \int_{-\infty}^{t_1} W(t_1, \tau_1) d\tau_1 \int_{-\infty}^{t_2} W(t_2, \tau_2)\, V_w(\tau_1) V_w(\tau_2) d\tau_2 \tag{6}$$

and average both sides over the ensemble of inputs $V_w(t)$ and we have

$$\phi_{yy}(t_1, t_2) = \int_{-\infty}^{t_1} W(t_1, \tau_1) d\tau_1 \int_{-\infty}^{t_2} W(t_2, \tau_2) \phi_{v_w v_w}(\tau_1, \tau_2) d\tau_2 \tag{7}$$

which is defined as the correlation function of the system output. Since the mean squared value of a random process can be obtained from the correlation function if $t_1 = t_2 = t$ we have

$$\langle Y^2(t) \rangle = \int_{-\infty}^{t} W(t, \tau_1) d\tau_1 \int_{-\infty}^{t} W(t, \tau_2) \phi_{v_w v_w}(\tau_1, \tau_2) d\tau_2 \tag{8}$$

where the brackets denote the time average and the mean squared value is a function of time (Reference 24).

Application of equation (8) to the flexible booster response problem is complicated by the fact that $V_w(t)$ in practice is a strongly nonstationary process primarily because of the large variations in vehicle velocity during launch. This effect can be more easily explained by considering α_g = angle of attack due to a gust input = $\frac{V_w}{V}$ which results in a large variation of α_g during launch. A given wind variation causes a larger α at low initial velocities than at a later time with corresponding higher velocity. The variations in dynamic pressure as they affect the input forces on the vehicle are assumed not to contribute to the input nonstationarity since these effects are included in the time varying vehicle model. This difficulty of the input process stationarity may be circumvented by assuming the spatial characteristics of the wind velocity profile to have local stationarity and that $V_w(t)$ can be approximated by a function of the form

$$V_w(t) = \int_{-\infty}^{t} \overline{V}_1(t_1)\, \overline{W}(t, t_1)\, dt_1$$

The process $\overline{V}_1(t_1)$ is assumed stationary and Gaussian and the weighting function $\overline{W}(t, \tau)$ serves to alter the white random process $\overline{V}_1(t)$ to give a function V_w with statistical properties similar to the non-stationary wind input and may be illustrated as shown on the following page.

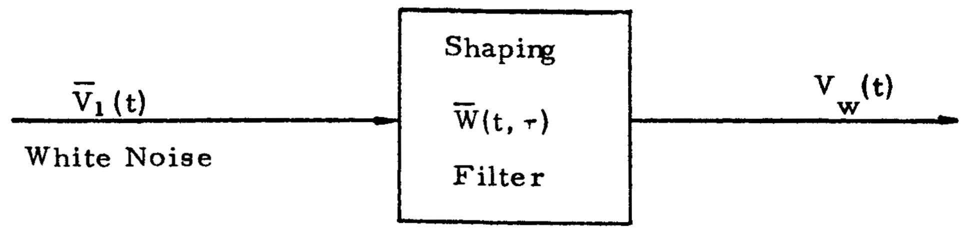

The next step is to obtain the overall system response as

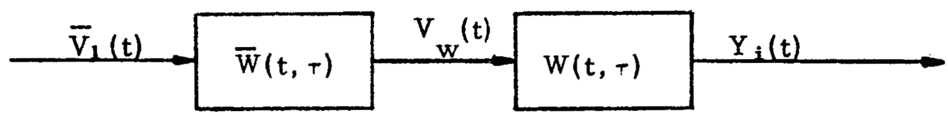

Combining $\overline{W}$ and W the total weighting filter - system weighting function is $W^*(t,\tau)$ and

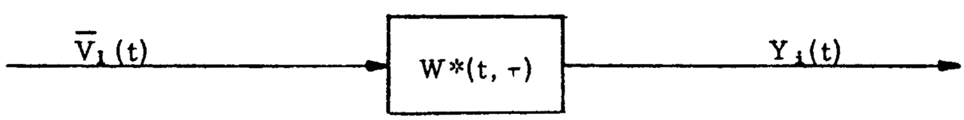

Now the system output correlation function becomes

$$\phi_{yy}(t_1, t_2) = \int_{-\infty}^{t_1} W^*(t_1, \tau_1)d\tau_1 \int_{-\infty}^{t_2} W^*(t_2, \tau_2)\phi_{v_1 v_1}(\tau_1, \tau_2)d\tau_2 \quad (9)$$

and the mean squared system output is

$$< Y^2(t) > = \int_{-\infty}^{t} W^*(t, \tau_1)d\tau_1 \int_{-\infty}^{t} W^*(t, \tau_2)\phi_{v_1 v_1}(t, \tau_2)d\tau_2 \quad (10)$$

Evaluation of (10) is a formidable task if performed directly but with the aid of adjoint analog techniques may be computed in a simple direct fashion for any value of t.

The correlation function $\phi_{\bar{V}_1 \bar{V}_1}(\tau)$ for the white random process $\bar{V}_1(t)$ is

$$\phi_{\bar{V}_1 \bar{V}_1}(\tau) = \delta(\tau)$$

and this simplification allows (10) to be reduced to a single integral as follows

$$\int_{-\infty}^{t} W^*(t, \tau_2)\, \delta(\tau_2 - \tau_1) d\tau_2 = W^*(t, \tau_1) \qquad (11)$$

and then

$$\langle Y^2(t) \rangle = \int_{-\infty}^{t} W^{*2}(t, \tau)\, d\tau \qquad (12)$$

where $W^*(t, \tau)$ is the weighting function for the composite weighting filter-vehicle system.

With the aid of the adjoint method (Reference 22) the composite system weighting function may be computed directly in a single run on an analog computer. This method for computing $W^*(t, \tau)$ is presented later in this discussion.

The mean squared system outputs computed by equation (12) are valid for a system which has been in operation for a long time before $t = 0$. In practice, the actual situation is that of a system initially at rest for all time $t < 0$. Some additional considerations are necessary for this case and will be discussed in a following section.

TIME-INVARIANT SYSTEM RESPONSE TO A STATIONARY PROCESS

A brief summary of the response of time-invariant systems to a stationary input process will be used to define system input-output relations which appear in example problems presented later in the text.

For a time invariant system $W(t, \tau_1)$ becomes a function of the time difference between application of the impulse, τ_1, and the time of observation, t. Thus, for this simplified case it may be written as $W(t-\tau_1) = W(\tau)$. The input-output system relation may be subsequently simplified so that the mean squared system output given by equation (10) becomes

$$<Y^2(t)> = \int_{-\infty}^{t} W^*(\tau_1)d\tau_1 \int_{-\infty}^{t} W^*(\tau_2)\phi_{v_1 v_1}(\tau_1 - \tau_2)d\tau_2 \tag{13}$$

If the input process is white noise then (13) reduces to

$$<Y^2(t)> = \int_{-\infty}^{t} \left[W^*(\tau)\right]^2 d\tau \tag{14}$$

For this simplified case the spectral characteristic of the output process can be determined by taking the Fourier transform of (9) as follows

$$G_{yy}(\omega) = \frac{1}{\pi} \int_{-\infty}^{\infty} \phi_{yy}(\tau) e^{-j\omega\tau} d\tau \tag{15}$$

Where $G_{yy}(\omega)$ is defined as the output spectral density. Equation (15) reduces to

$$G_{yy}(\omega) = \left|Y(j\omega)\right|^2 G_{xx}(\omega) \tag{16}$$

where $Y(j\omega)$ is the system transfer function and $G_{xx}(\omega)$ is the Fourier Transform of the input correlation function.

The mean squared system output (variance) may be defined as

$$\begin{aligned} \langle Y^2(t) \rangle &= \int_0^\infty G_{yy}(\omega)\, d\omega \\ &= \int_0^\infty \left|Y(j\omega)\right|^2 G_{xx}(\omega)\, d\omega \end{aligned} \tag{17}$$

for a stable system. The standard deviation, σ, of the output process is the square root of the variance.

There is some special consideration necessary for systems which begin operation at a finite time and have output statistics which change with time. This can happen either during starting transients or for systems which have some instabilities. These systems require transient statistical analysis techniques which are discussed in some detail in Reference 24.

Determination of the System Weighting Function by the Adjoint-Analog Method

The adjoint method for determining the response of a linear time varying system to white Gaussian noise was developed by Laning and Battin and is described in Reference 22 and Reference 24. This technique is one of the major contributions to analog computer art in recent years. The weighting function of a time varying system of linear differential equations can be computed by one analog computer run by using this method.

The adjoint differential equations of a set of linear differential equations are defined by equation (18) and (19) as follows (Reference 22).

Linear Differential and Supplementary Algebraic Equations

$$\frac{d}{dt} X_i(t) = a'_{ip}(t)\, X_p(t) + a'_{i\alpha}(t) X_\alpha(t) + b'_i(t)\, f(t)$$

$$X_j(t) = b_{j\lambda}(t)\, X_\lambda(t) + b'_j(t)\, f(t) \tag{18}$$

$$i, p, \lambda = 1, 2, \ldots, m$$

$$\alpha = m+1, \ldots, n$$

$$m < j \leq n$$

Modified Adjoint System

$$\frac{d}{d\bar{t}} Y_k(\bar{t}) = Y_p(\bar{t})\, a'_{pk}(t_2 - \bar{t}) + Y_\alpha(\bar{t})\, a'_{\alpha k}(t_2 - \bar{t}) - g_k(\bar{t})$$

$$Y_j(\bar{t}) = Y_\lambda(\bar{t}) b_{\lambda j}(t_2 - \bar{t}) \tag{19}$$

$$\overline{w}_r(t_2 - \bar{t}, t_2) = Y_1 b'_1 + \ldots + Y_m b'_m$$

$$k, p, \lambda = 1, 2, \ldots, m$$

$$j, \alpha = m+1, \ldots, n$$

The weighting function for the linear equations equals $\overline{W}_{r'}(t_2, t_1)$ which is the weighting function for the adjoint system. A time scale transformation $\bar{t}=t_2 - t$ has been introduced into the adjoint system to permit direct computation of $w(t_1, t_2)$. Consider a system with the weighting function $w(t_1, t_2)$ shown below:

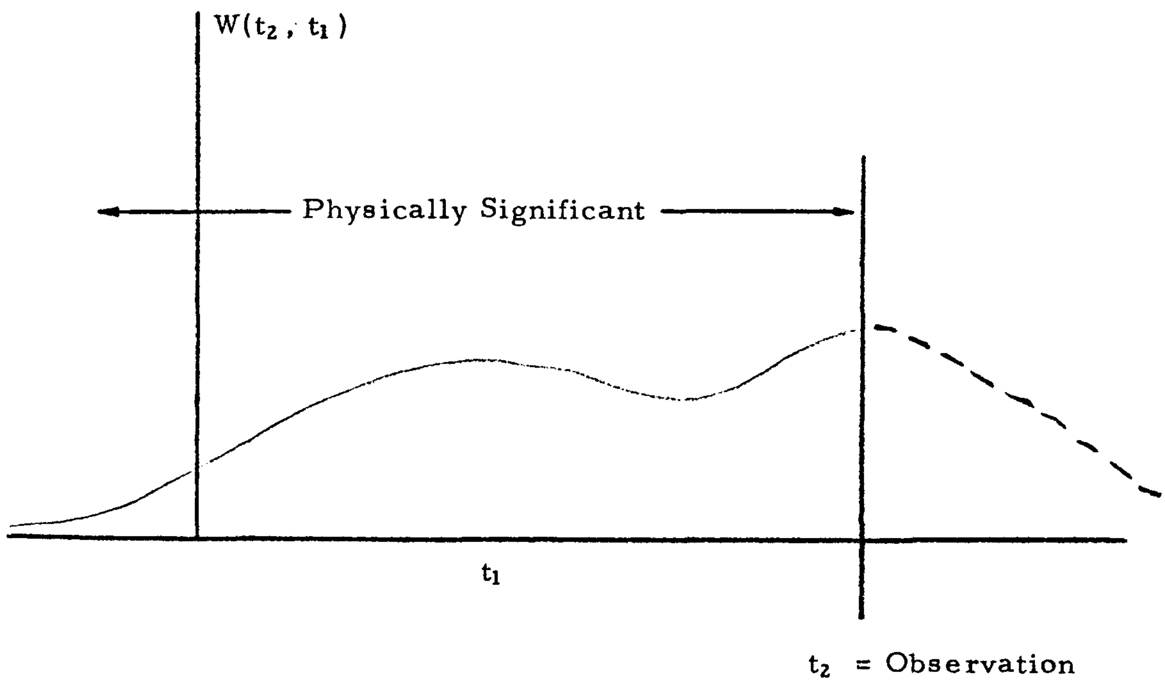

then the adjoint system weighting function is

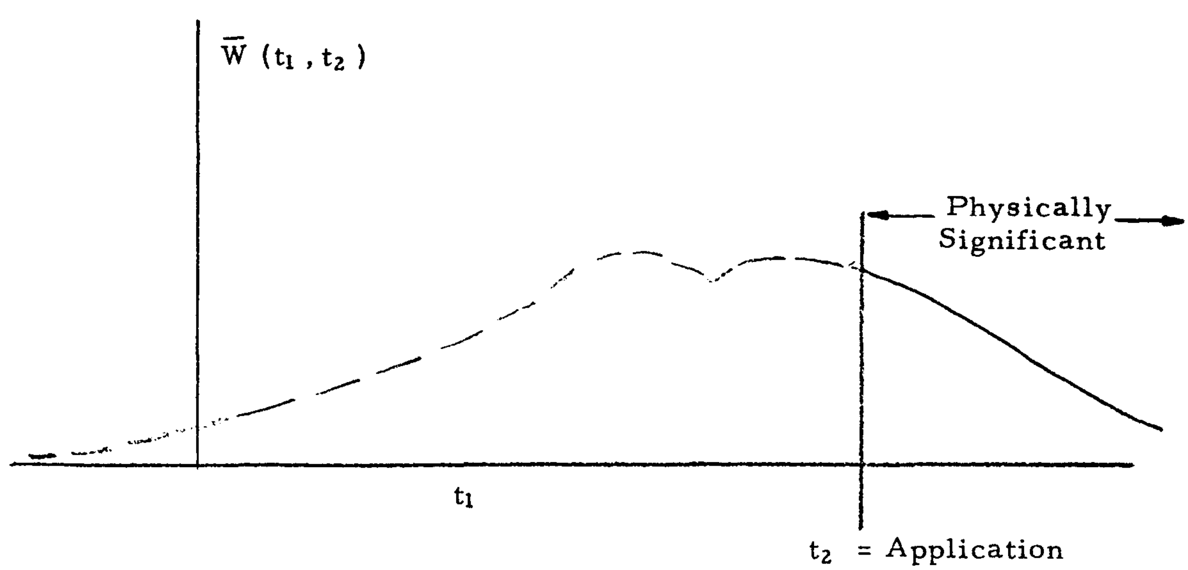

Introduction of the time scale change $\bar{t} = t_2 - t$ into the adjoint system results in the modified adjoint system and $w(t_2 - \bar{t}, t_2)$ is

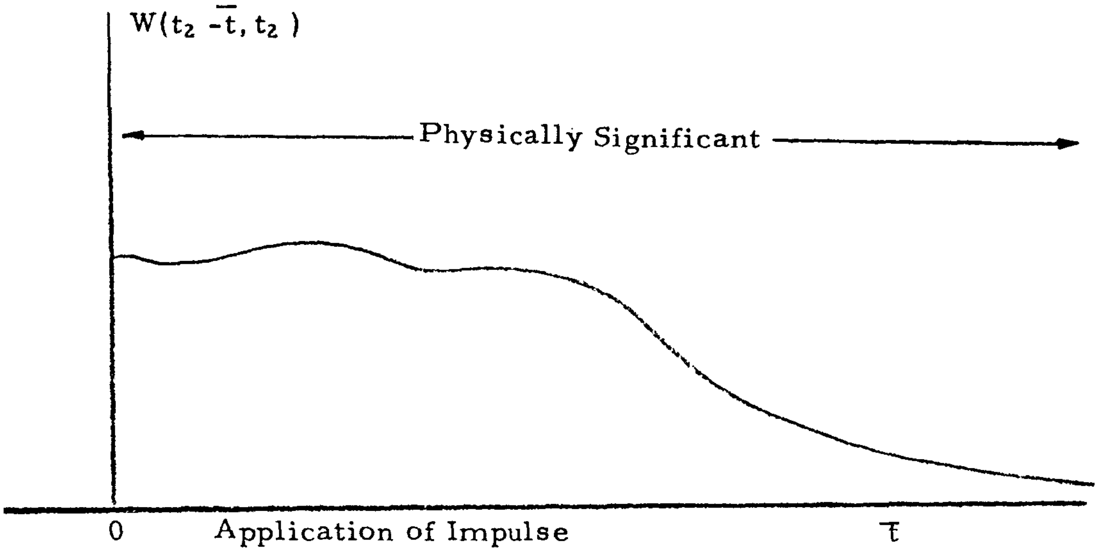

Although the concept and mathematics of the modified adjoint system are quite complex the analog diagram of the modified adjoint system may be obtained in a simple, straightforward manner as follows:

1. The inputs to the system analog become the outputs of the adjoint analog.
2. The outputs of a summer or integrator become the inputs to that amplifier in the adjoint analog.
3. The input and output are exchanged on all potentiometers.
4. Potentiometers which are used to represent the time varying coefficients are replaced by multipliers driven by the coefficient as a function of the new variable $\bar{t} = t_2 - t$, i. e., time varying coefficients are started at their final values and run backward.

5. A unit impulse is put into the integrator from which the output of interest was taken in the system analog. The impulse input may be simulated by initial conditions on the proper integrators.
6. The adjoint weighting function is measured, in the adjoint analog at the points where the corresponding inputs in the system analog were introduced.

This technique may be illustrated by considering an example problem consisting of a simplified rigid vehicle model described by the equations 1 through 6 which follow

1. $I(t)\ddot{\phi} = -F_s X_E \beta - Q F_1 (t) \alpha$
2. $m(t)\ddot{Y} = (F-X) \phi + F_s \beta + Q F_o(t) \alpha$
3. $\beta = a_o(t) \phi + a_1 (t) \dot{\phi} + g_2 (t) A_2$
4. $\alpha = \phi - \dfrac{\dot{Y}}{v} + \dfrac{v_w}{v}$
5. $A_1 = \ddot{Y} - g(t) \phi =$
6. $BM = M'_\beta(t) \beta + M'_\alpha(t) \alpha$

These equations may be put in the form of equation (19) if the following substitutions are made:

$$\dot{\phi} = P \quad , \quad \ddot{\phi} = \dot{P}$$

$$\dot{Y} = V \quad , \quad \ddot{Y} = \dot{V}$$

This transformation of equations is not necessary if the rules previously stated are followed. It is of interest however to begin with the form of equation (19). Equations 1 through 6 may be written as follows with the aid of the preceeding substitutions -

1. $\dot{P} = - \frac{F_s X_E}{I} \beta - \frac{QF_1}{I} \alpha$

2. $\dot{q} = P$

3. $\dot{V} = \frac{F-X}{m} q + \frac{F_s}{m} \beta + \frac{QF_o}{m} \alpha$

4. $\beta = a_o q + a_1 P + g_2 A_i$

5. $\alpha = q - \frac{V}{v} + \frac{v_w}{v}$

6. $A_i = \dot{V} - g q$

7. $BM = M'_\beta \beta + M'_\alpha \alpha$

By algebraic substitution we will make the supplementary algebraic equations (4, 5, 6, 7) function of only the integrator output variables p, q, and V. The equations which result are in the form of equation (18) and are expressed in the matrix form as shown on the following page.

$$
\begin{bmatrix} p \\ q \\ v \\ \beta \\ \alpha \\ BM \end{bmatrix}
=
\begin{bmatrix}
0 & 0 & 0 & a_{14} & a_{15}(t) & 0 \\
a_{21} & 0 & 0 & 0 & 0 & 0 \\
0 & a_{32} & 0 & a_{34} & a_{35}(t) & 0 \\
a_{41} & a_{42}(t) & a_{43}(t) & 0 & 0 & 0 \\
0 & a_{52} & a_{53}(t) & 0 & 0 & 0 \\
a_{61} & a_{62} & a_{63} & 0 & 0 & 0
\end{bmatrix}
\begin{bmatrix} p \\ q \\ v \\ \beta \\ \alpha \\ BM \end{bmatrix}
+
\begin{bmatrix} 0 \\ 0 \\ 0 \\ a_4(t) \\ a_5(t) \\ a_6(t) \end{bmatrix}
\begin{bmatrix} V_w \end{bmatrix}
$$

where:

$$a_{14} = -\frac{F_s X_E}{I}$$

$$a_{15} = -\frac{QF_1}{I}$$

$$a_{21} = 1$$

$$a_{32} = \frac{F-X}{m}$$

$$a_{34} = \frac{F_s}{m}$$

$$a_{35} = \frac{QF_o}{m}(t)$$

$$a_{41} = \frac{g_2 F_s a_1}{m\left(1 - \frac{F_s g_2}{m}\right)} + a_1$$

$$a_{42} = g_2 \frac{\left(\frac{F-X}{m} - g + \frac{QF_o}{m} + \frac{F_s}{m} a_o\right)}{1 - \frac{F_s g_2}{m}} + a_o$$

$$a_4 = \frac{g_2 QF_o}{mv}\left(\frac{1}{1 - \frac{F_s g_2}{m}}\right)$$

$$a_5 = \frac{1}{v} \qquad a_6 = \frac{M'_\beta g_2 \left(\frac{QF_o}{mv}\right)}{1 - F_s g_2/m} + \frac{M'_\alpha}{v}$$

$$a_{43} = -g_2 \frac{QF_o}{mv}\left(\frac{1}{1 - \frac{F_s g_2}{m}}\right)$$

$$a_{52} = 1$$

$$a_{53} = -\frac{1}{v}$$

$$a_{61} = \frac{M'_\beta g_2 F_s a_1}{m - F_s g_2} + M'_\beta a_1$$

$$a_{62} = M'_\beta g_2 \frac{\left(\frac{F-X}{m} - g + \frac{QF_o}{m} + \frac{F_s a_o}{m}\right)}{1 - F_s g_2/m} + M'_\beta a_o + M'_\alpha$$

$$a_{63} = M'_\beta \left(\frac{-g_2 QF_o}{mv}\right)\left(\frac{1}{1 - \frac{F_s g_2}{m}}\right) - \left(\frac{M'_\alpha}{v}\right)$$

The Direct System Analog Diagram is shown in Figure 1 and the Adjoint System in Figure 2.

Finally the modified adjoint equations derived from the analog diagram are

$$\begin{bmatrix} \dot{p}^* \\ \dot{q}^* \\ \dot{v}^* \\ \beta^* \\ \alpha^* \end{bmatrix} = \begin{bmatrix} 0 & a_{21} & 0 & a_{41} & 0 \\ 0 & 0 & a_{32} & a_{42} & a_{52} \\ 0 & 0 & 0 & a_{43} & a_{53} \\ a_{14} & 0 & a_{34} & 0 & 0 \\ a_{15} & 0 & a_{35} & 0 & 0 \end{bmatrix} \begin{bmatrix} p^* \\ q^* \\ v^* \\ \beta^* \\ \alpha^* \end{bmatrix} + \begin{bmatrix} a_{61} \\ a_{62} \\ a_{63} \\ 0 \\ 0 \end{bmatrix} \begin{bmatrix} BM^* \end{bmatrix}$$

$$w\ (t_2 - t_1, t_2) = a_4 \beta^* + a_5 \alpha^* + a_6\ BM^*$$

$$= \text{Modified Adjoint System}$$

BM Weighting Function

DEFINITION OF THE WIND INPUT SPECTRA

The adjoint method provides a means of computing directly the weighting function for a time varying system - weighting filter combination, therefore mean square system outputs can be easily obtained for a time varying system responding to a nonstationary input. The only restriction is that the fundamental input process, i.e., the weighting filter input, be stationary, Gaussian, white noise.

Now let us formulate an atmospheric turbulence model that will be used as the problem input. The essential ingredients are shown in the following block diagram.

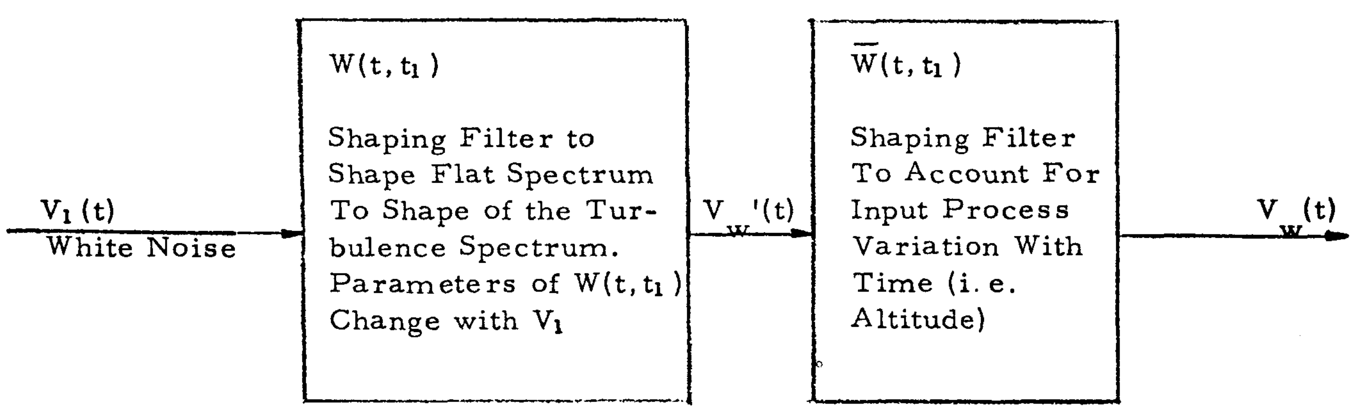

To provide more insight into the input process description let us consider a simple problem neglecting $W(t, t_1)$. Assume that the horizontal wind velocity characteristics with altitude are described by

$$\phi_{v_w}(\Omega) = \frac{\sigma_w^2 L}{\pi} \; \frac{1+3L^2\Omega^2}{(1+\Omega^2 L^2)^2}$$

which is recognized as the Press atmospheric turbulence power spectra model. Ω is the spatial frequency in radians per meter, L is the scale of the turbulence, and σ_w^2 is the variance of the process. At altitudes below 50,000 feet this spectra has proved to be a good model of the vertical and horizontal atmospheric turbulence characteristics. The process has been shown to be approximately Gaussian and locally stationary, References 3 and 13. Application to the problem at hand is complicated, however, because $\Omega = \frac{\omega}{V}$ where V is the vehicle velocity and w is the circular frequency in radians per second. In other words the spectrum shape changes with vehicle velocity. With the adjoint method this presents no problem, however, and does not restrict the model.

The weighting filter is constructed using methods described in Reference 24. The spectra

$$\phi_{v_w}\left(\frac{\omega}{V}\right) = \frac{\sigma_w^2 L}{\pi} \quad \frac{1+3L^2\left(\frac{\omega}{V}\right)^2}{\left[1+\left(\frac{\omega}{V}\right)^2 L^2\right]^2}$$

may be factored and written in the form

$$\phi(\omega) = H_1(\omega)\,\overline{H_1(\omega)}$$

where

$$H_1(\omega) = \sigma_w\sqrt{\frac{L}{\pi V}} \quad \frac{1+\sqrt{3}\,L\left(\frac{j\omega}{V}\right)}{\left[1+L\left(\frac{j\omega}{V}\right)\right]^2}$$

$$\overline{H_1}(\omega) = \sigma_w\sqrt{\frac{L}{\pi V}} \quad \frac{1-\sqrt{3}\,L\left(\frac{j\omega}{V}\right)}{\left[1-L\left(\frac{j\omega}{V}\right)\right]^2}$$

The weighting filter characteristics necessary to shape a white noise spectrum to the spectrum shape

$$\phi_{V_w}(\omega) = \frac{\sigma_w^2 L}{\pi V} \frac{1 + 3L^2\left(\frac{\omega}{V}\right)^2}{\left[1 + \left(\frac{\omega}{V}\right)^2 L^2\right]^2}$$

is

$$Y(j\omega) = \sigma_w \sqrt{\frac{L}{\pi V}} \frac{1 + \sqrt{3}\, \frac{L}{V}\, (j\omega)}{\left[1 + \frac{L}{V}(j\omega)\right]^2}$$

or in Laplace transform notation

$$\frac{V_w(s)}{I(s)} = Y(s) \doteq K \frac{1 + \sqrt{3}\, \frac{L}{V}\, s}{\left[1 + \frac{L}{V}(s)\right]^2}$$

where I(s) is the input

Inverse transforming gives

$$\frac{L^2}{V^2} \int \ddot{V}_w \, dt = K \int i(t)\, dt + K \int \sqrt{3}\, \frac{L}{V} \left(\frac{di}{dt}\right) dt - 2\frac{L}{V} \int \frac{dV_w}{dt}\, dt - \int V_w(t) dt$$

as the integrodifferential equation that defines the weighting filter. Now if we let the vehicle velocity vary we have an equation of the form

$$a_1(t) \frac{dV_w(t)}{dt} = K(t) \int i(t)\, dt + K(t)\sqrt{3}\frac{L}{V(t)}\, i(t) - 2\, \frac{L}{V(t)}\, V_w(t) - \int V_w(t) dt$$

with time varying coefficients. This differential equation modifies the assumed stationary white noise input, i(t), to give a good approximation of the actual non-stationary input process to the vehicle.

Implicit in the statistical representation of the horizontal wind data is the averaging of the wind profile data over an infinite (large number) ensemble of wind data. The frequency content (spectra) may vary considerably over long periods of time and weather conditions. The dilemma, of which input data to use should cease to exist as more data,reduced as nonstationary data in the proper format, becomes available. Present applications favor a spectra obtained by averaging the spectra for many profiles and excluding any spectra obtained during highly unusual conditions when operations would be cancelled anyway. New techniques for the spectral analysis of nonstationary processes are outlined in detail in Reference 25. Application of methods outlined in the above reference report would result in a process description that could be easily simulated by the adjoint method.

The data presented by Scoggins (Reference 13) indicates a high degree of stationarity in the higher frequency range and his data correlates well with past atmospheric turbulence models at high frequencies. A comparison of Scoggins results with the Press model spectra is shown in Figure 3 for a vehicle velocity of 525 m/sec. The vertical scatter of the Scoggins data is shown approximately in Figure 3. The Press spectra is shown for two values of L = 304 and 1000 meters. It is felt that the value of L = 1000 is more representative of the scale of the lateral turbulence encountered in this problem. Also the spectra presented herein would not give a valid simulation of very long wavelength variations in the input process, i.e. larger than 10 kilometer wavelengths.

APPLICATION TO A SATURN V MODEL

In order that some of the principles which have been previously reviewed can be demonstrated an example problem which illustrates the major points of this analysis is presented. The simplified Saturn V mathematical model described in equation (1) is used as a basis for a simple investigation of the role of accelerometer feedback in alleviating load and reducing drift. The assumptions and conditions for the problem are as follows

1. The systems are assumed to have constant coefficients with values determined at time = 80 seconds
2. The system input is a lateral wind, V_w, only
3. The wind input is assumed stationary and to have a power spectrum as shown in Figure 3, i.e., the Press spectra for L = 304, σ = 1.414; L = 1000, σ = 2.5
4. The vehicle model is assumed to simulate (a) rigid body rotation and translation, (b) gimbal dynamics, (c) accelerometer dynamics and (d) one bending mode.
5. Only rigid body bending moment as determined by the mode acceleration method is considered.

For this simplified model the mean squared bending moment and lateral drift can be determined by

$$<Y^2_{BM}(t)> = \int_0^t \left[W^*_{BM}(\tau)\right]^2 d\tau$$

and

$$<Y^2_{\dot{y}}(t)> = \int_0^t \left[W^*_{\dot{y}}(\tau)\right]^2 d\tau$$

where $W^*_{BM}(t)$ and $W^*_{\dot{y}}(t)$ are the composite bending moment and lateral drift weighting filter weighting function respectively as defined previously. For this particular case the weighting function can be solved for directly from the system equations instead of the modified adjoint equations because of the non-time-varying character of this example problem. However all of the principles of the adjoint method are illustrated by this problem.

The implementation of the adjoint analog simulation is described in Appendix A. The system outputs which are recorded are

1. All important system outputs are recorded as a function of time. Items recorded are BM, α, $\dot{y}$, β, ϕ, and $V_w(t)$.
2. The value of $\langle Y^2_{BM}(t)\rangle$ and $\langle Y^2_{\dot{y}}(t)\rangle$ for a particular time (for a stable system after $\langle Y^2_{\dot{y}}(t)\rangle$ and $\langle Y^2_{BM}(t)\rangle$ have stabilized.

It should be noted that the primary analog simulation outputs were the composite system-weighting filter impulsive responses. The actual system, $V_w(t)$, input was the output of the weighting filter. Figure 4 shows the weighting filter response to a unit impulse for two values of L. It should be noted that the larger the value of L, the longer the input, $V_w(t)$, into the system persists. The actual system response to a real unit impulse would have a memory time of less than 10 seconds, however, for values of L larger than 1000, the psuedo-impulse input to the system could persist at sizeable values for almost ten seconds. A simple interpretation of this result is that the combined system memory time is effectively increased by input processes with a large low frequency content as in this problem.

A typical system response to the weighting filter output for L = 304, σ = 1.414 is illustrated in Figure 5. Control system gains are a_1 = 1.1, a_o = .48, g_2 = .039, i.e., nominal values. This particular configuration has near critical rigid body damping. Most of the oscillation evident in the gimbal angle time history is due to gimbal dynamics and bending. Notice how the lateral drift quickly returns to zero for this set of system gains. The first bending mode is excited at a very low level by the psuedo-wind impulse and has only a small contribution to the mean squared bending moment. The reader is reminded at this time that $<Y^2_{BM}(t)>$ and $<Y^2_{\dot{y}}(t)>$ are computed by squaring and integrating the $\dot{y}$ and BM time responses shown in Figure 5.

Figure 6 illustrates the changes in the BM weighting function as accelerometer gain, g_2, varies. The change in rigid body dynamics as g_2 is varied color the results, slightly. The more oscillatory response obtained for higher values of g_2 cause a larger mean square value than the well damped response characteristics obtained as gain is lowered. A similar set of $\dot{Y}$ weighting functions is presented in Figure 7. The main point of interest here is that as g_2 is lowered the value of $\dot{Y}$ ceases to return to zero and either becomes divergent or has a constant bias as time becomes large. Because of the characteristic response of $\dot{Y}$ the mean square value must be determined for a given time (10 seconds) since the value of the integral of $W^*_{\dot{y}}(t)^2$ gets large with time. In other words this value must be interpreted as the transient statistical response. Figure 8 and 9 illustrate the effect of L on the bending moment and lateral drift weighting functions. Comparison of these two figures shows that the difference is primarily evident in the initial part of $W^*_{BM}(t)$ and $W^*_{\dot{y}}(t)$.

It is interesting to compare the values of 3σ bending moment and lateral drift for various control system gain variations. The 3σ values of BM and $\dot{Y}$ may be interpreted as values of these quantities which will be exceeded approximately 1 percent of the time, i.e., 99 percent values. Figure 10 shows the effect of accelerometer gain on the 3σ value of bending moment at Station 25. The effect of a_1 and a_o are also indicated. Figure 11 illustrates effects of these same parameter variations on 3σ values of lateral drift and Figure 12 illustrates the effect of adding one bending mode and accelerometer location changes on the subject model. The effect on 3σ bending moment at Station 25 due to the addition of one bending mode is minor. Only rigid vehicle bending moment is computed in this study and variations in the 3σ bending moment are primarily due to decreased stability of some modes which cause larger gimbal excursions which contribute greatly to rigid vehicle bending moment.

Figures 13 and 14 illustrate the effect of α and $\dot{Y}$ feedback on the system response characteristics. It can be seeen that the α meter feedback is very similar to accelerometer feedback but is not quite as sensitive to gain changes; $\dot{Y}$ feedback is of little value, primarily because of lateral drift instabilities incurred.

The effect of increases in turbulence scale factor L are presented in Figure 15. Increase in L (a measure of the average effective length of the turbulence wavelengths) causes large increase in vehicle bending moment response, i.e., the vehicle is sensitive to long wavelength disturbances which contribute significantly to the vehicle response.

CONCLUSIONS AND RECOMMENDATIONS

An overall consideration of the results of this analysis supports the statistical approach used in the analysis. It is evident that the nonstationary system response of a large flexible booster can be described successfully with the techniques presented in this report. There are several areas where considerable theoretical and experimental work remains to be done (such as the input process definition), however, it is felt that the feasibility of this method is proved and the implementation of a general, time varying, adjoint model is obtainable with a relatively small effort.

The major conclusions which may be drawn from this report are:

1. The adjoint-analog technique is applicable to the large booster vehicle wind response problem and can yield accurate results with very small amounts of data processing and computer run time.
2. The complete time varying character of the problem can be retained, however, the present analysis will not apply if system nonlinearities exist.
3. The character of the nonstationary input process is retained.
4. The variance of all system outputs is easily obtainable.
5. The lateral wind input process can be described by the application of advanced nonstationary process theory to the wind profile data reduction problem.
6. Implementation of the adjoint-analog simulation on a modern high-speed analog computer offers a means of system optimization and

parameter investigation which would be unsurpassed in speed and flexibility.

The recommendations which results from this study are:

1. Further investigation of the input weighting-function system adjoint is believed to be warranted for the nonstationary system model. This preliminary evaluation of the method has proved the major claims which have been made for the adjoint method in the past.

2. In view of the low level of effort, in the past, directed to the problem of obtaining a time varying spectral representation of the input process it is strongly recommended that more effort be made in this area. This preliminary investigation has indicated several approaches to this problem.

3. Extension of the method to include the nonlinearity in the bending moment equation due to nonlinear aerodynamics is highly desirable. Preliminary investigations indicate the feasibility of this modification.

REFERENCES

1. Hinich, Melvin J., "Spectral Estimation of Nonstationary Noise by Means of a Parametric Model," AIAA Paper No. 65-235.

2. Low, George M., "The Compressible Laminar Boundary Layer with Fluid Injection," NACA Technical Note 3404.

3. Press, Harry, "Atmospheric Turbulence Environment with Special Reference to Continuous Turbulence," Report No. 115, Advisory Group for Aeronautical Research and Development, April-May 1957.

4. Henry, Robert M., "A Statistical Model for Synthetic Wind Profiles for Aerospace Vehicle Design and Launching Criteria," NASA Technical Note D-1813, July 1963.

5. Allan G. Piersol, "The Measurement and Interpretation of Ordinary Power Spectra for Vibration Problems," NASA CR-90, September 1964.

6. Scoggins, James R., and Vaughan, William W., "Cape Canaveral Wind and Shear Data (1 through 80 KM) for Use in Vehicle Design and Performance Studies," NASA Technical Note D-1274, July 1962.

7. Johnson, Walter A., McRuer, Duane T., and Phatak, Anil V., "Extension of Linear Constant-Coefficient Analysis Methods to Time Varying Systems," RTD-TDR-63-4178, Systems Technology, Inc., September 1964.

8. Reed, Wilmer H., III, "Models for Obtaining Effects of Ground Winds on Space Vehicles Erected on the Launch Pad," Virginia Polytechnic Institute; Blacksburg, Virginia, August 17-21, 1964.

9. Lappe, U. Oscar, "A Low Altitude Turbulence Model for Estimating Gust Loads on Aircraft,", AIAA Paper No. 65-14.

10. Rechtien, Richard D., "The Autocorrelation Function of Structural Response Measurements," NASA Technical Note D-2578, January 1965.

11. Leybold, Herbert A., "Techniques for Examining Statistical and Power Spectral Properties of Random Time Histories," NASA Technical Note D-2714, March 1965.

12. Townsend, Don, "Saturn V Wind Response Studies," MTP-AERO-63-63, 10 September 1963, Marshall Space Flight Center.

13. Scoggins, James R., and Vaughan, William W., "Some Properties of Atmospheric Turbulence for Space Vehicles," Aerospace Environment Office, Aero Astrodynamics Laboratory, NASA-MSFC, June 1965.

14. Goldman, Robert, "A Method for Predicting Dynamic Response of Missiles to Atmospheric Disturbances," IAS Paper No. 62-40.

15. Diederich, Franklin W., "The Dynamic Response of a Large Airplane to Continuous Random Atmospheric Disturbances," IAS Report, Vol. 23, No. 10, October 1956.

16. Mazzola, Luciano L., "Design Criteria for Wind-Induced Flight Loads on Large Boosted Vehicles," AIAA Report, Vol. 1, No. 4, April 1963.

17. Lester, Harold C., and Morgan, Homer G., "Determination of Launch Vehicle Response to Detailed Wind Profiles," AIAA Paper, January-February 1965.

18. Morgan, Homer G., and Collins, Dennis F., Jr., "Some Applications of Detailed Wind Profile Data to Launch Vehicle Response Problems," AIAA Paper, February 1963.

19. Bieber, R. E., "Missile Structural Loads by Nonstationary Statistical Methods," IAS Paper, April 1961.

20. Bendat, J. S., <u>Principles and Applications of Random Noise Theory</u>, John Wiley and Sons, Inc., New York. 1958.

21. Crandall, Stephen H., <u>Random Vibration</u>, Vol. 2, The M.I.T. Press, Cambridge, Massachusetts, 1963.

22. Fifer, Stanley, <u>Analogue Computation</u>, McGraw-Hill Book Company, Inc., 1961, Vol. IV.

23. Enochson, Loren D., "Frequency Response Functions and Coherence Functions for Multiple Input Linear Systems," NASA Report CR-32, April 1964.

24. Laning and Battin, <u>Random Processes in Automatic Control</u>, McGraw-Hill Company, Inc., 1956.

25. Bendat and Others, "Advanced Concepts of Stochastic Processes and Statistics for Flight Vehicle Vibration Estimation and Measurement," ASD-TDR-62-973, 1962.

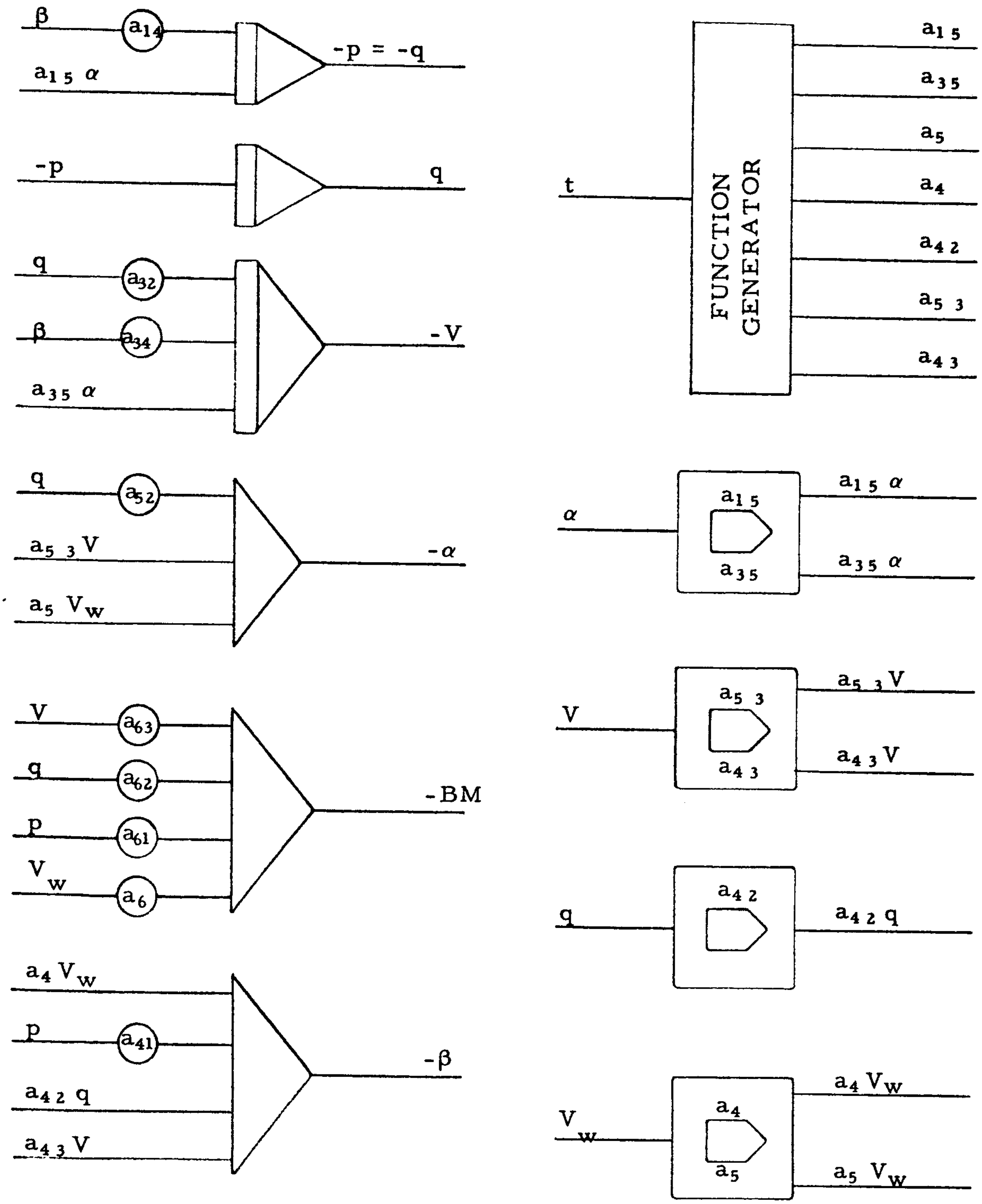

FIGURE 1 DIRECT ANALOG DIAGRAM

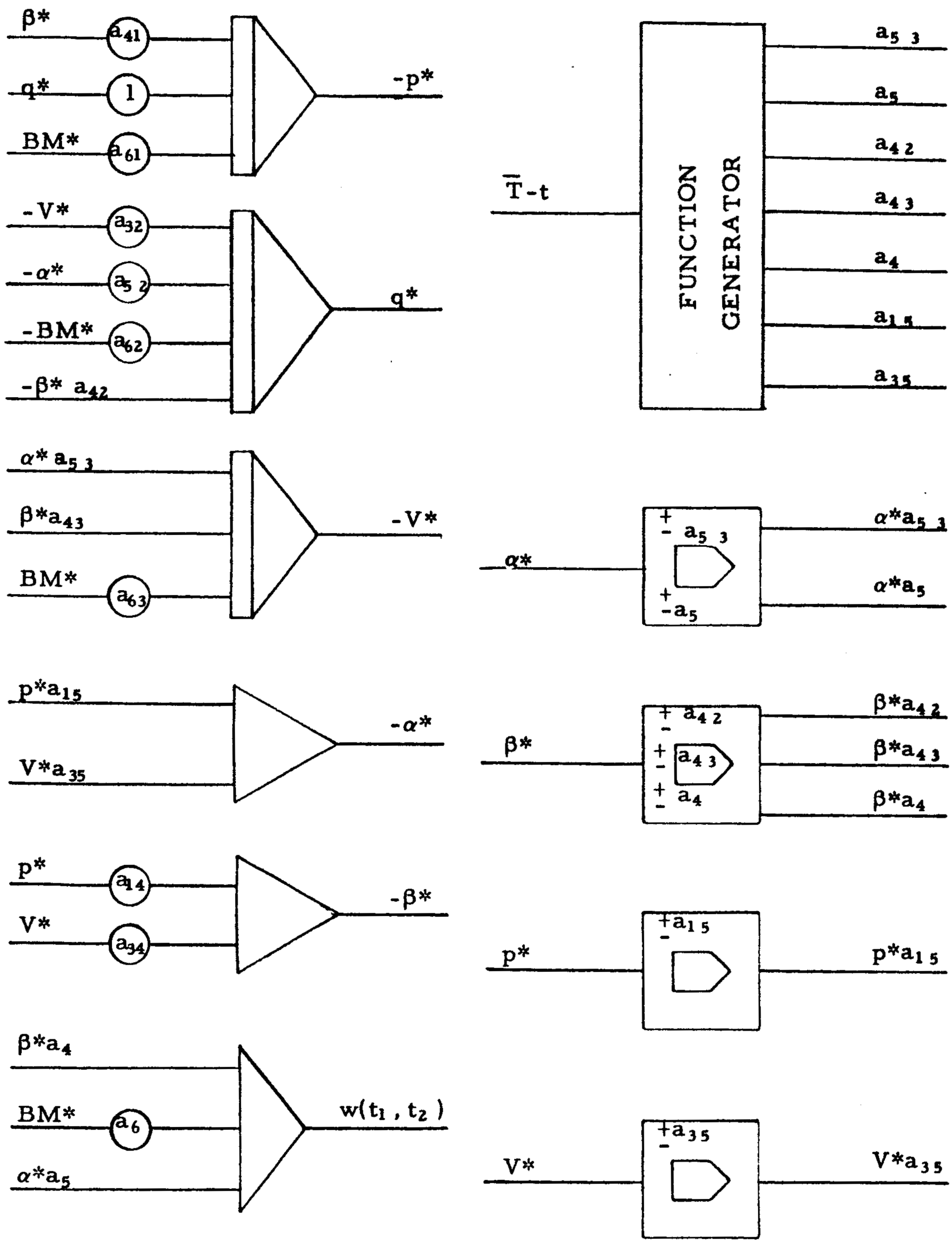

FIGURE 2 ADJOINT ANALOG DIAGRAM

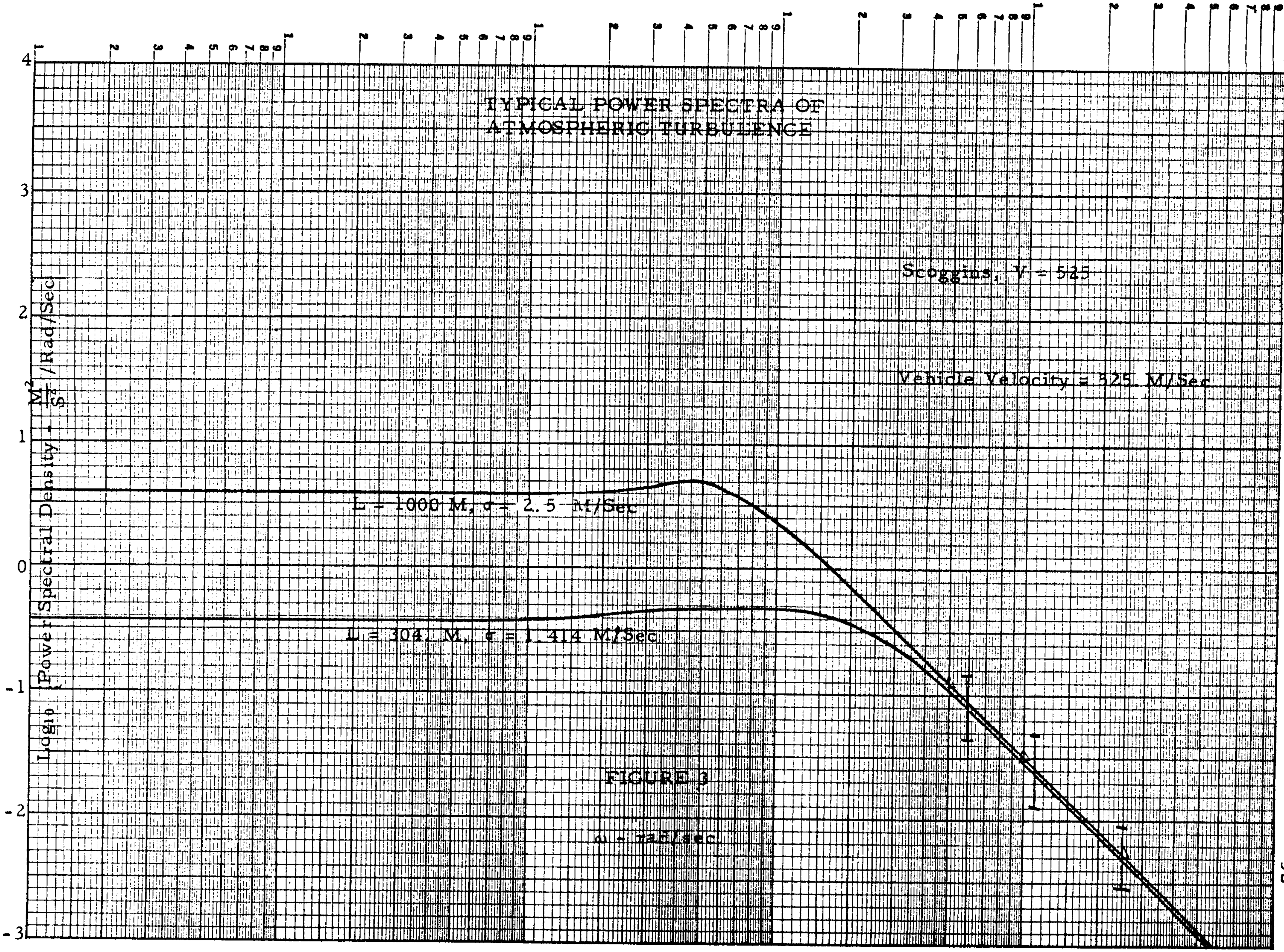
TYPICAL POWER SPECTRA OF
ATMOSPHERIC TURBULENCE
Scoggins, V = 525
Vehicle Velocity = 525 M/Sec
L = 1000 M, σ = 2.5 M/Sec
L = 304. M, σ = 1.414 M/Sec
Log10 Power Spectral Density - M²/S² /Rad/Sec
ω - rad/sec
4
3
2
1
0
-1
-2
-3

FIGURE 3

WEIGHTING FILTER RESPONSE TO
AN UNIT IMPULSE

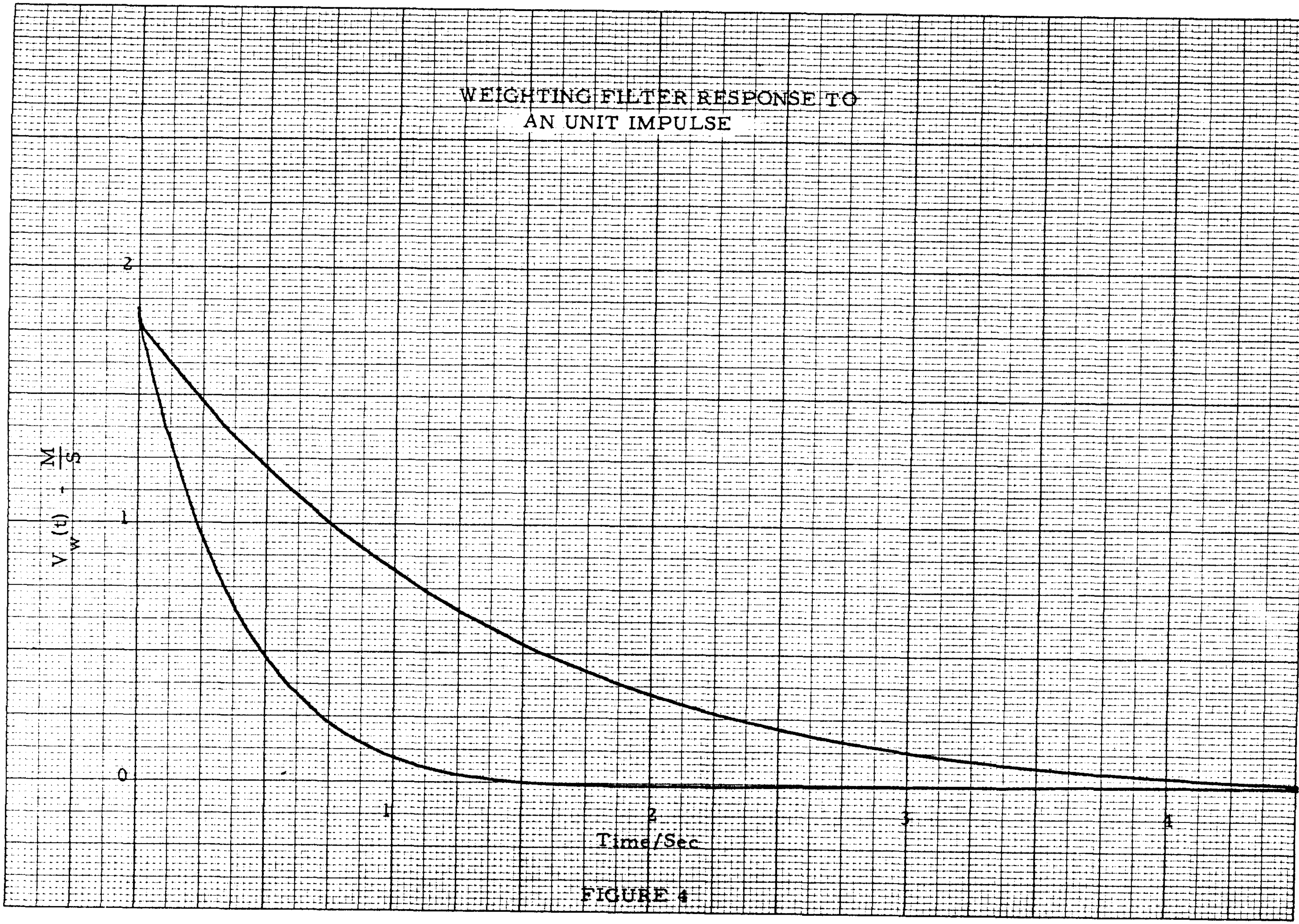

FIGURE 4

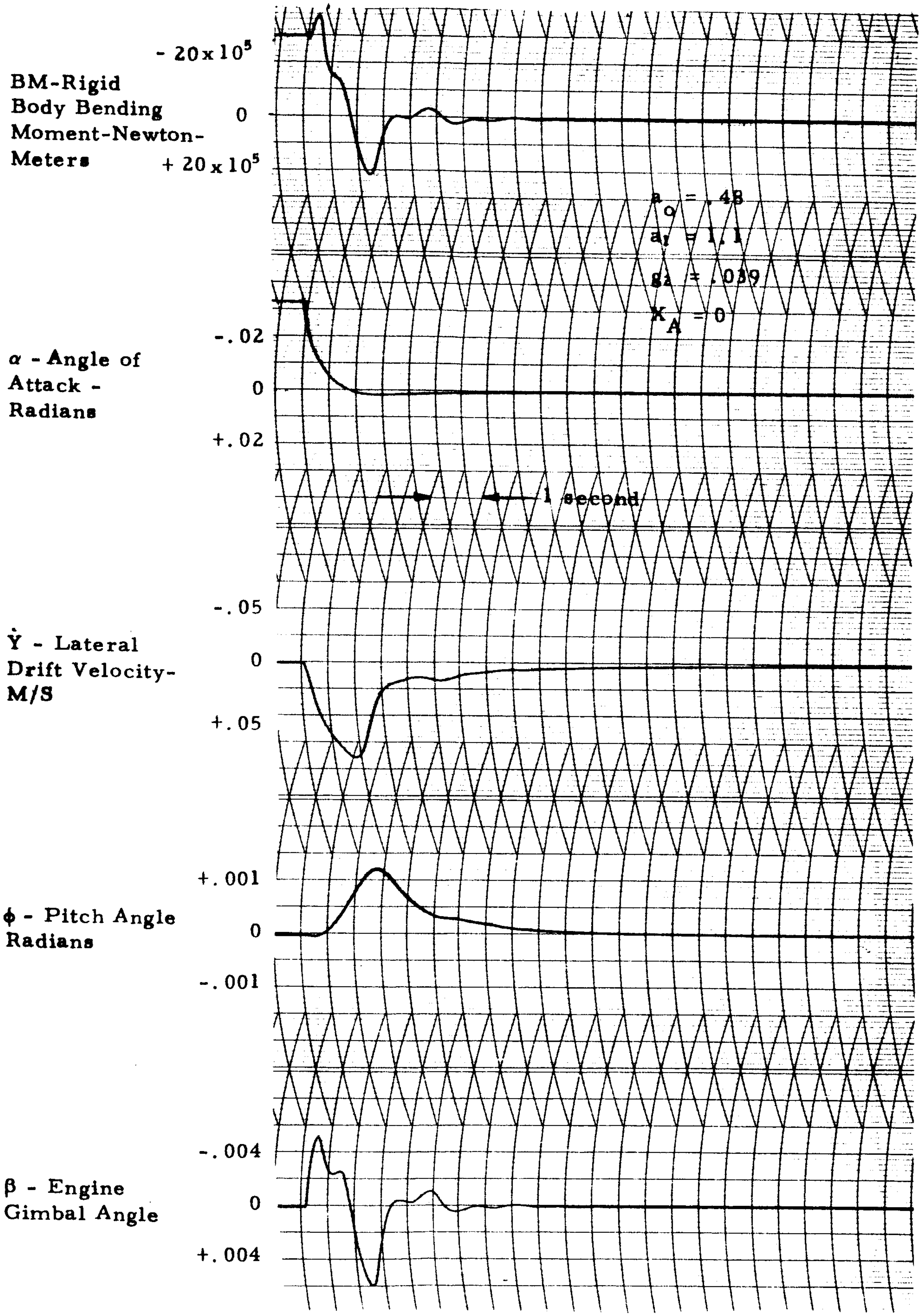

TYPICAL SYSTEM-WEIGHTING FUNCTION
RESPONSE TO A 10 x UNIT IMPULSE

FIGURE 5

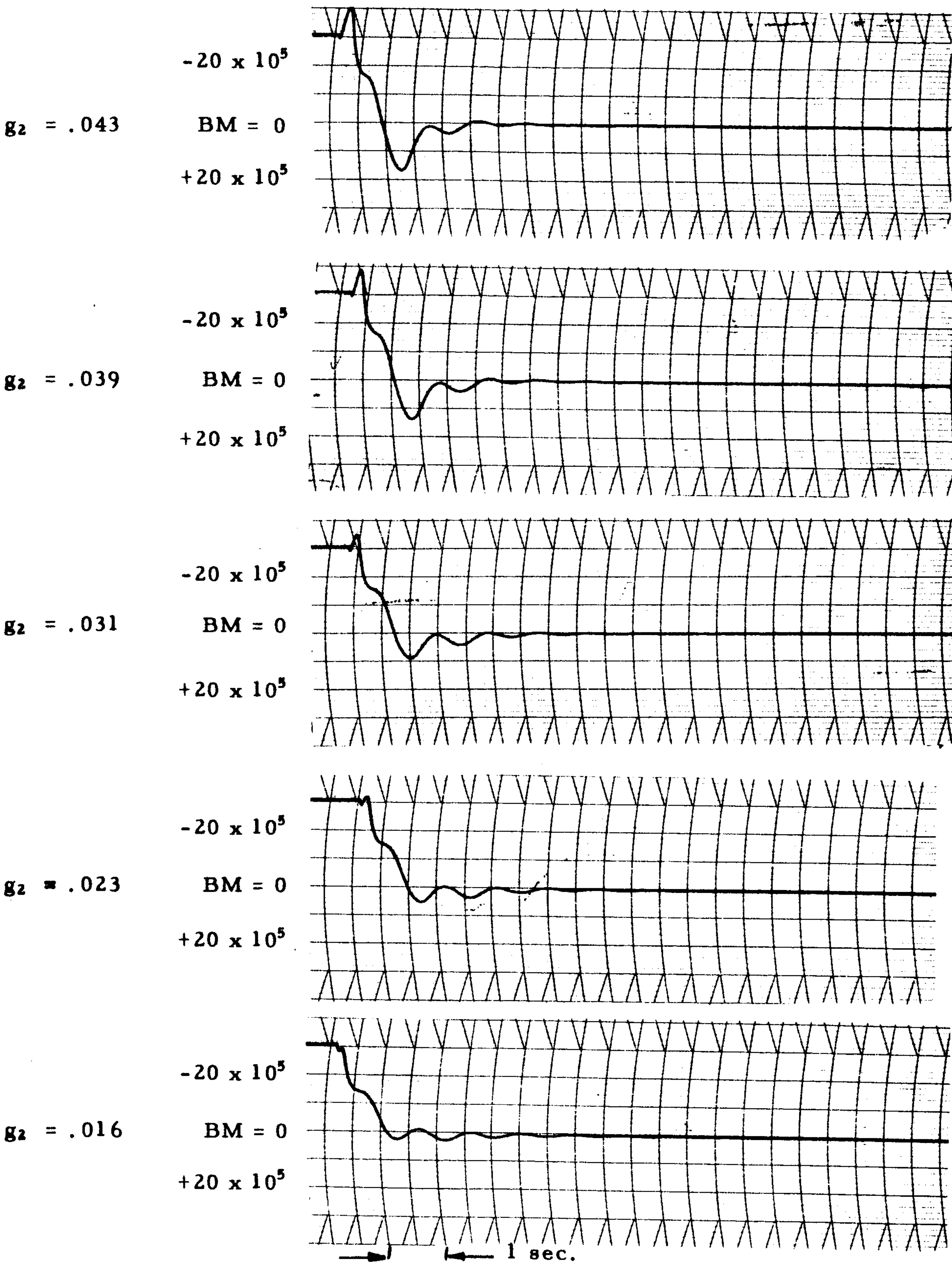

BENDING MOMENT WEIGHTING FUNCTIONS -
EFFECT OF VARIATION IN ACCELEROMETER GAIN g_2
(ONE BENDING MODE, GIMBAL DYNAMICS, $X_A = -5$)

FIGURE 6

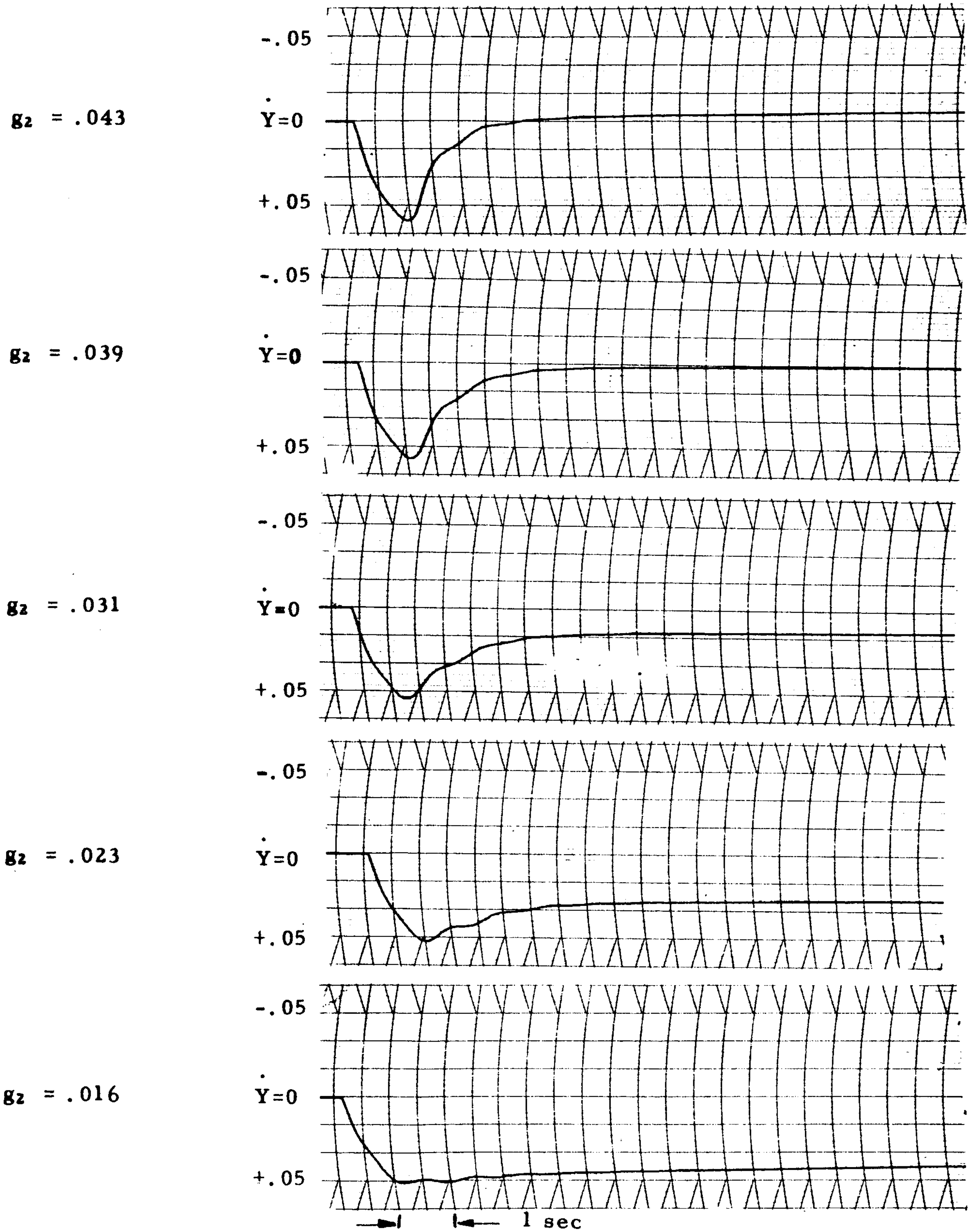

LATERAL DRIFT WEIGHTING FUNCTIONS -
EFFECT OF VARIATION IN ACCELEROMETER GAIN g_2
(ONE BENDING MODE, GIMBAL DYNAMICS, X_A=-5)

FIGURE 7

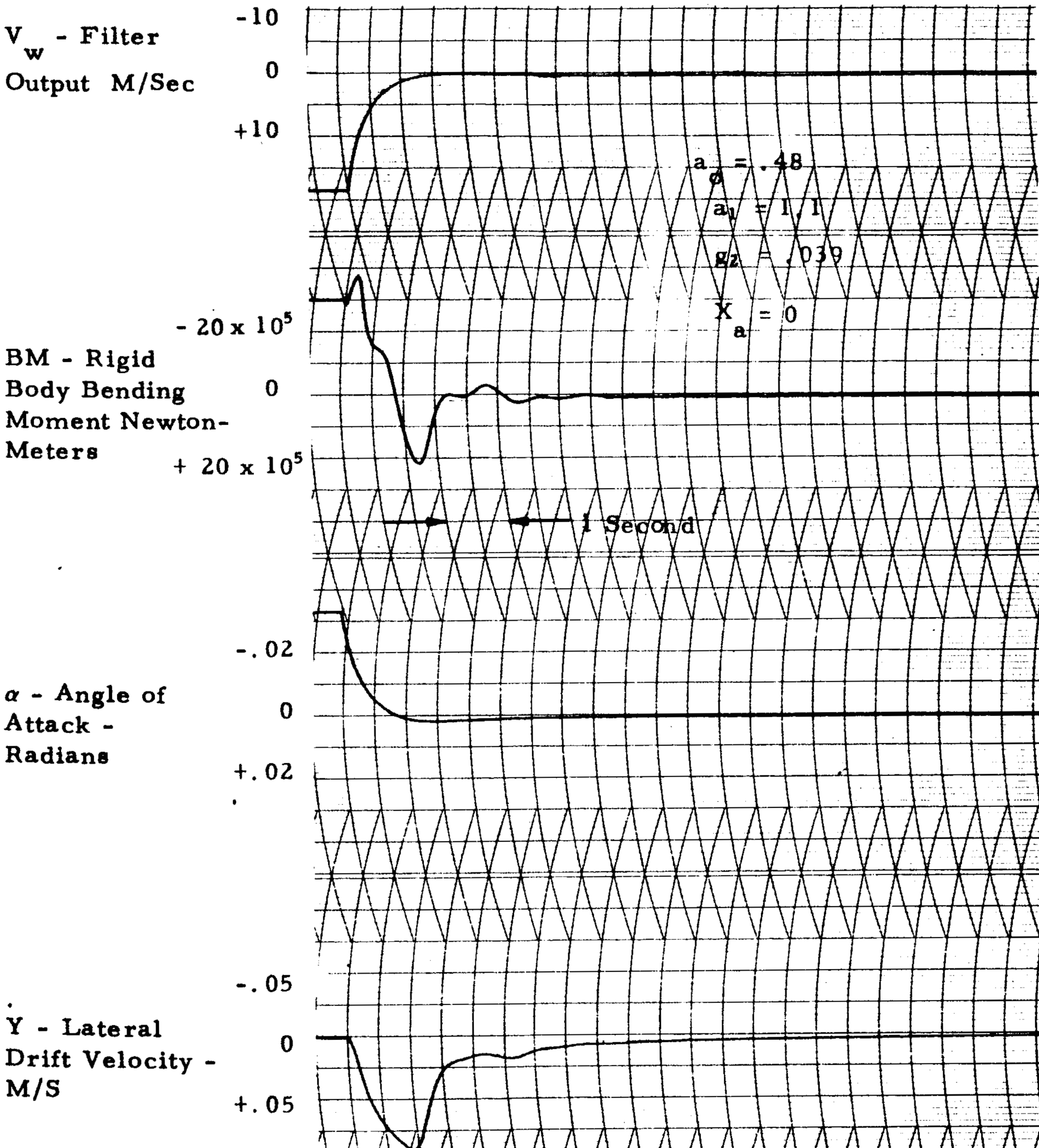

EFFECT OF TURBULENCE SCALE FACTOR L
ON SYSTEM WEIGHTING
L = 304

FIGURE 8

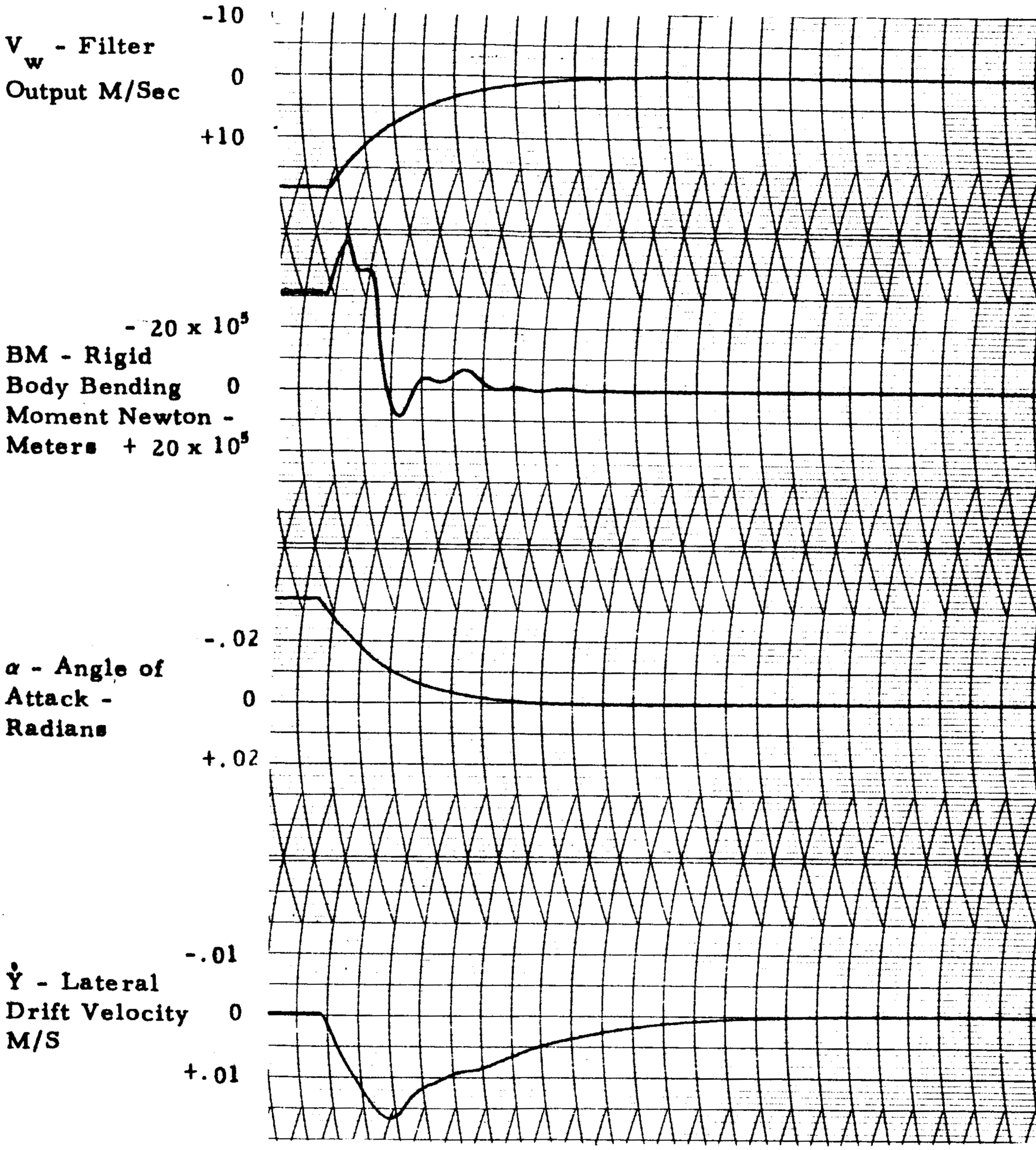

EFFECT OF TURBULENCE SCALE FACTOR L
ON SYSTEM WEIGHTING
L = 1000

FIGURE 9

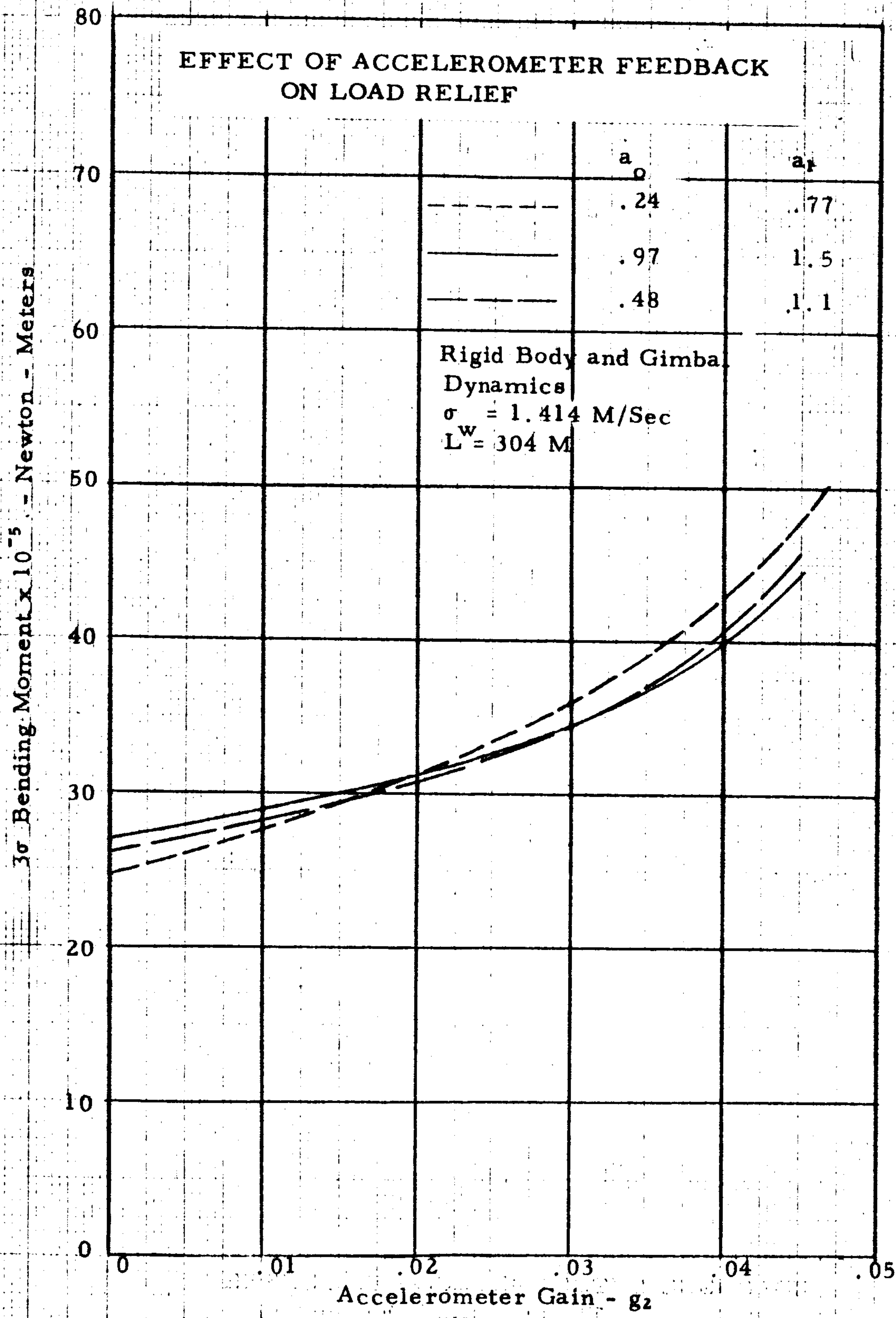
EFFECT OF ACCELEROMETER FEEDBACK
ON LOAD RELIEF
a_o
a_1
.24
.77
.97
1.5
.48
1.1
Rigid Body and Gimbal
Dynamics
σ_w = 1.414 M/Sec
L = 304 M
3σ Bending Moment x 10^{-5} - Newton - Meters
80
70
60
50
40
30
20
10
0
0
.01
.02
.03
.04
.05
Accelerometer Gain - g_2

FIGURE 10

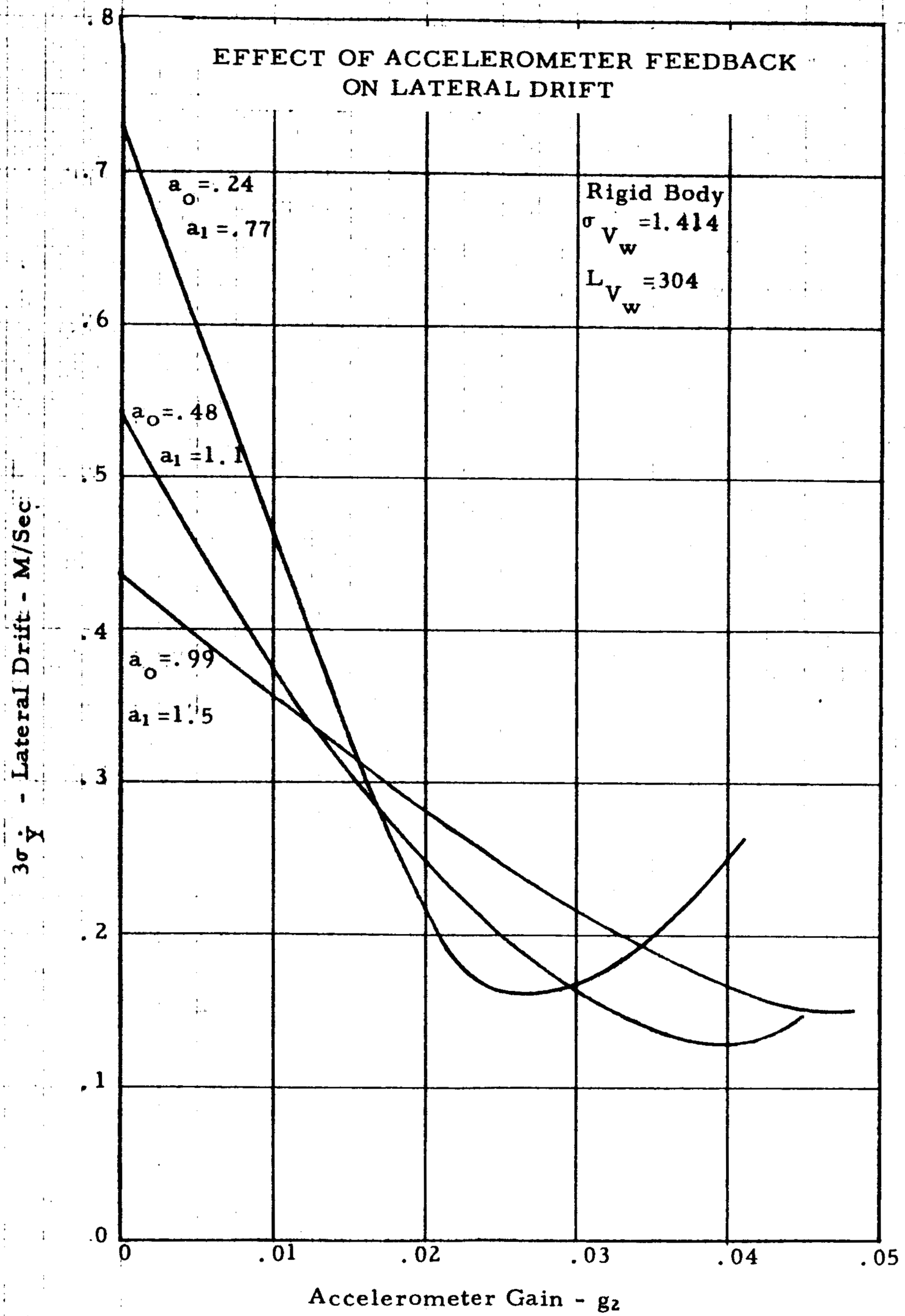
EFFECT OF ACCELEROMETER FEEDBACK
ON LATERAL DRIFT
Rigid Body
$\sigma_{V_w} = 1.414$
$L_{V_w} = 304$
$a_o = .24$
$a_1 = .77$
$a_o = .48$
$a_1 = 1.1$
$a_o = .99$
$a_1 = 1.5$
$3\sigma_{\dot{Y}}$ - Lateral Drift - M/Sec
.8
.7
.6
.5
.4
.3
.2
.1
.0
0
.01
.02
.03
.04
.05
Accelerometer Gain - g_2

FIGURE 11

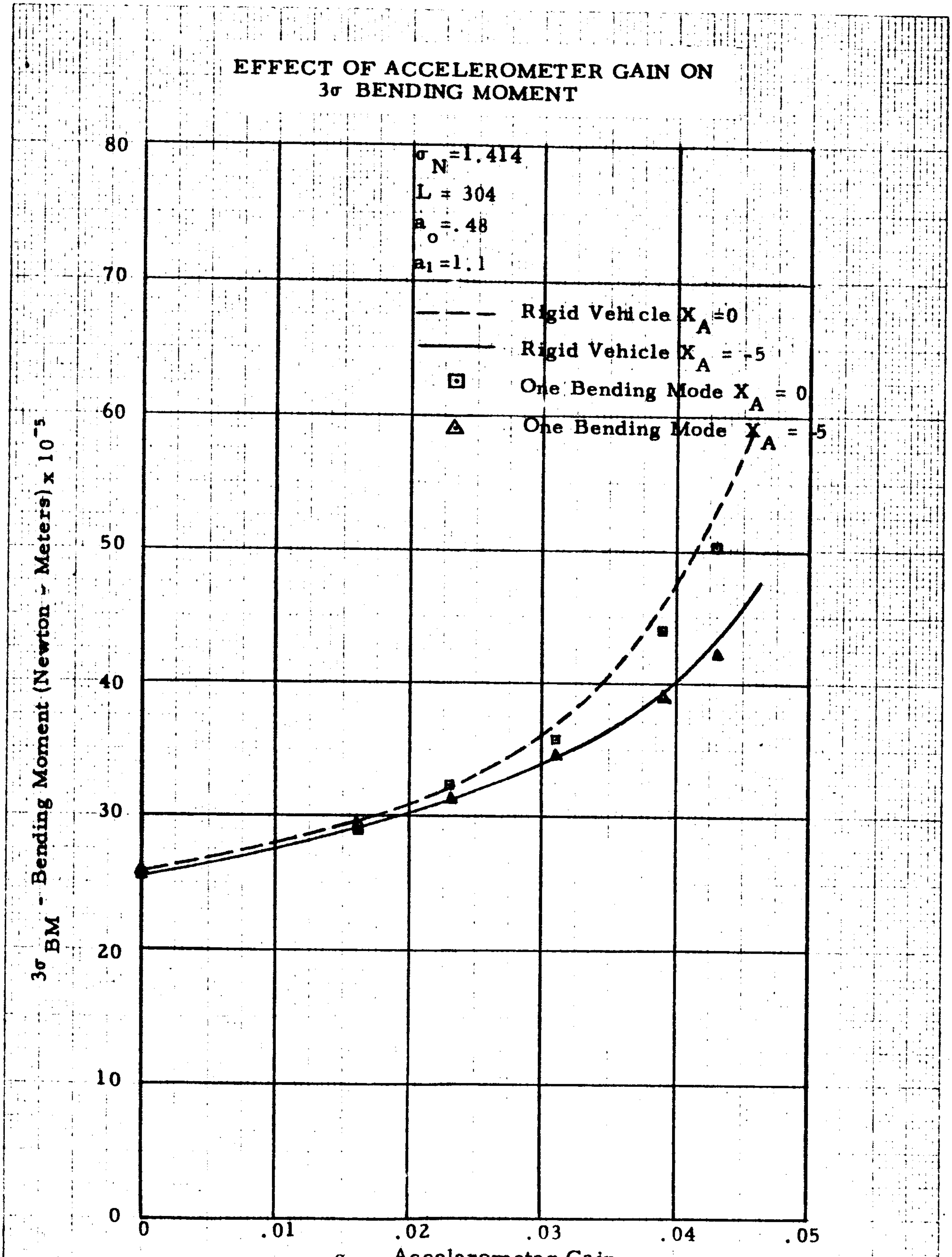
EFFECT OF ACCELEROMETER GAIN ON
3σ BENDING MOMENT
$\sigma_N = 1.414$
$L = 304$
$a_o = .48$
$a_1 = 1.1$
Rigid Vehicle $X_A = 0$
Rigid Vehicle $X_A = -5$
One Bending Mode $X_A = 0$
One Bending Mode $X_A = -5$
$3\sigma_{BM}$ - Bending Moment (Newton - Meters) x 10^{-5}
80
70
60
50
40
30
20
10
0
0
.01
.02
.03
.04
.05
g_2 - Accelerometer Gain

FIGURE 12

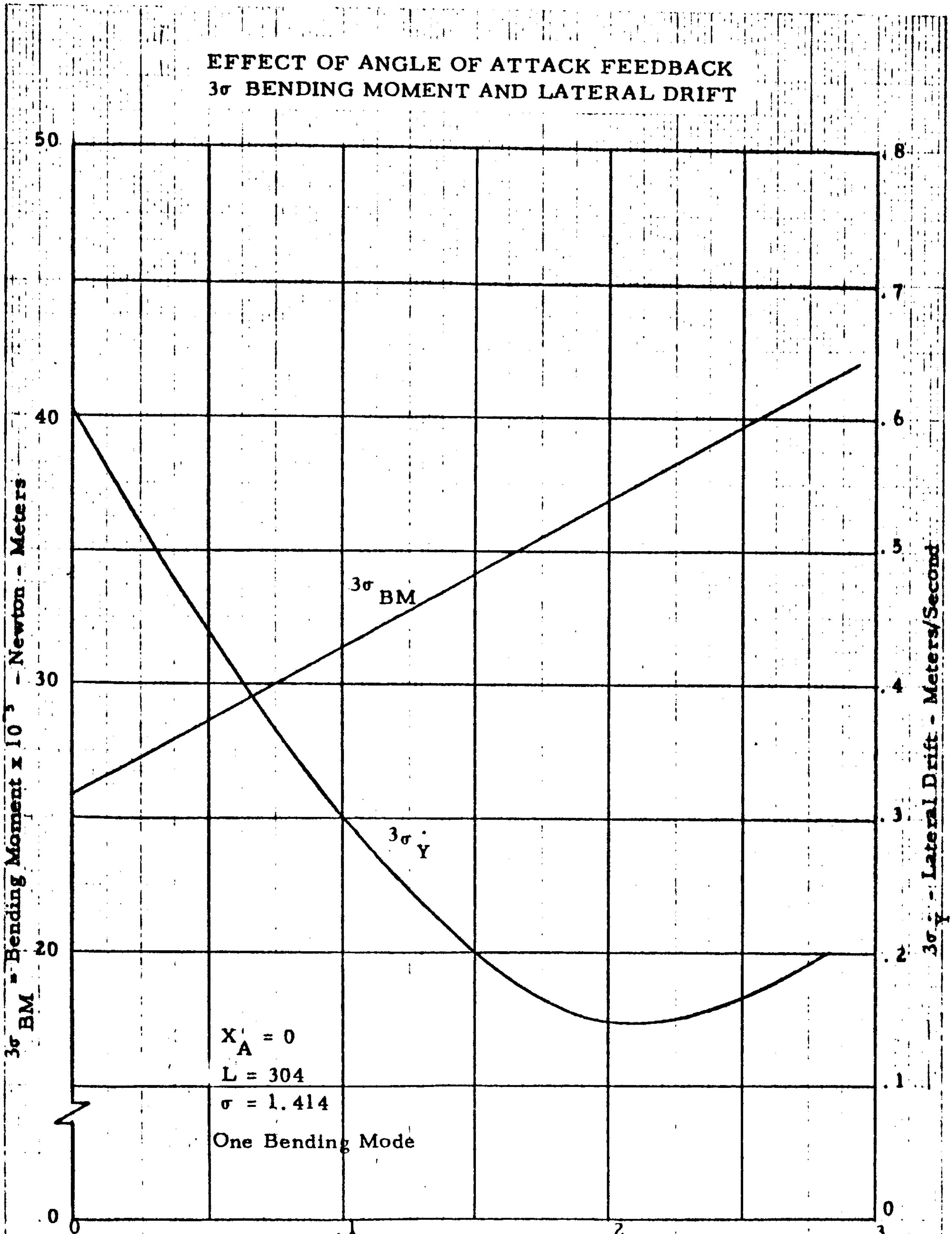

g_4 - α Control Loop Gain

FIGURE 13

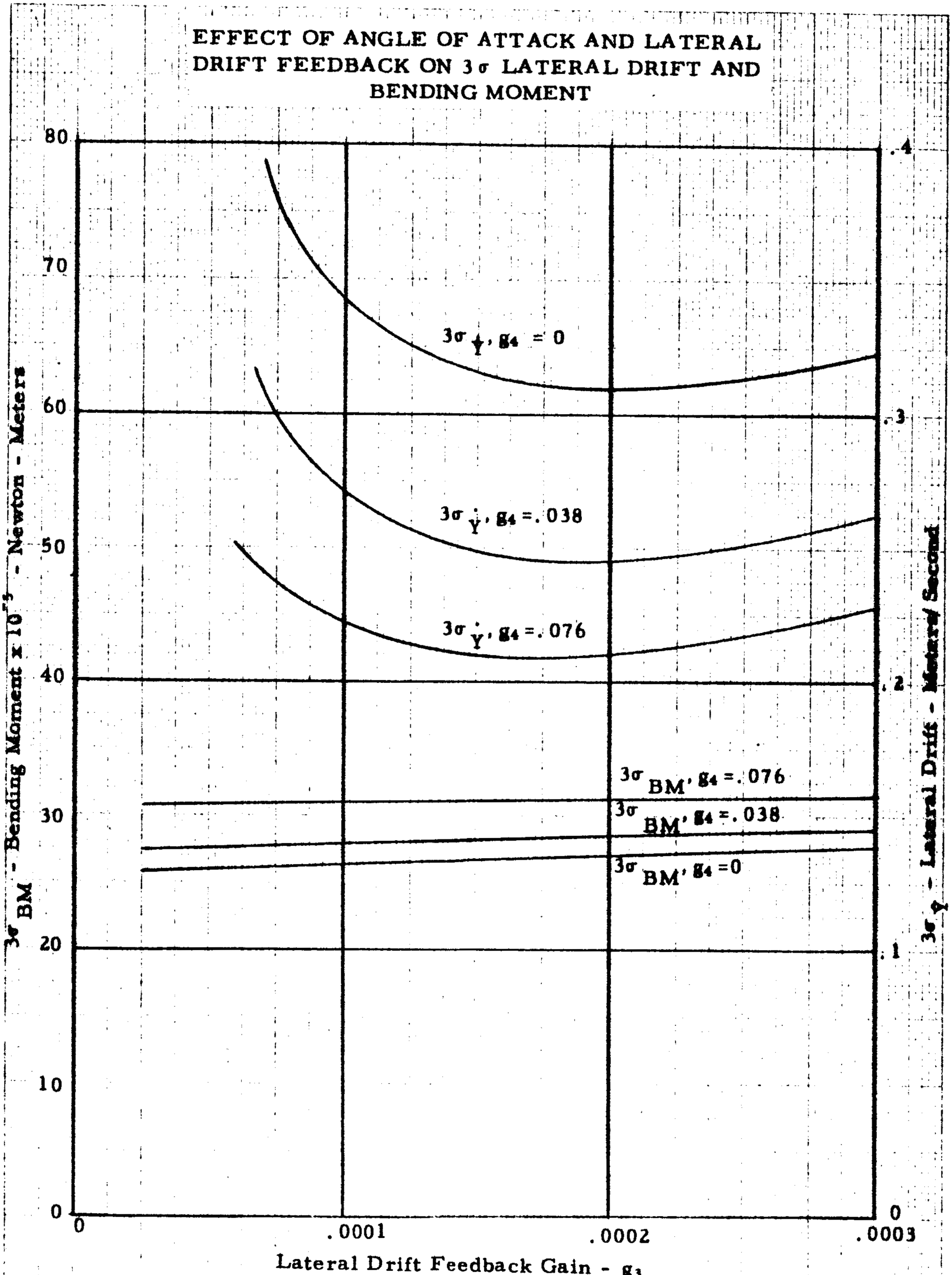

EFFECT OF ANGLE OF ATTACK AND LATERAL DRIFT FEEDBACK ON 3σ LATERAL DRIFT AND BENDING MOMENT
80
70
60
50
40
30
20
10
0
.4
.3
.2
.1
0
0
.0001
.0002
.0003
$3\sigma_{\dot{Y}}$, g_4 = 0
$3\sigma_{\dot{Y}}$, g_4 = .038
$3\sigma_{\dot{Y}}$, g_4 = .076
$3\sigma_{BM}$, g_4 = .076
$3\sigma_{BM}$, g_4 = .038
$3\sigma_{BM}$, g_4 = 0
$3\sigma_{BM}$ - Bending Moment x 10^{-5} - Newton - Meters
$3\sigma_{\dot{Y}}$ - Lateral Drift - Meters/ Second
Lateral Drift Feedback Gain - g_3

FIGURE 14

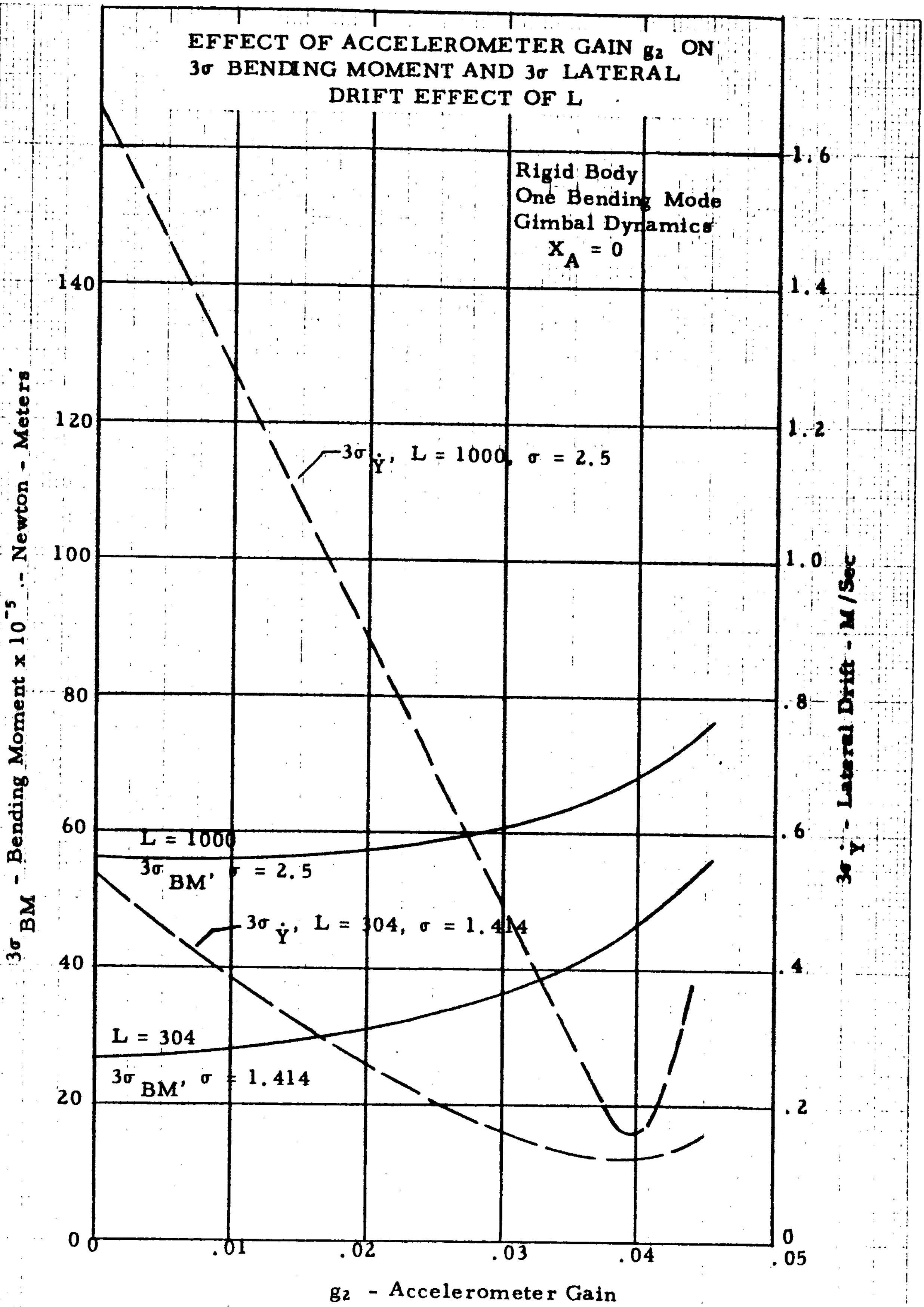
EFFECT OF ACCELEROMETER GAIN g2 ON
3σ BENDING MOMENT AND 3σ LATERAL
DRIFT EFFECT OF L
Rigid Body
One Bending Mode
Gimbal Dynamics
X_A = 0
3σ_Ẏ, L = 1000, σ = 2.5
L = 1000
3σ_BM, σ = 2.5
3σ_Ẏ, L = 304, σ = 1.414
L = 304
3σ_BM, σ = 1.414
140
120
100
80
60
40
20
0
1.6
1.4
1.2
1.0
.8
.6
.4
.2
0
.01
.02
.03
.04
.05
3σ_BM - Bending Moment x 10^-5 - Newton - Meters
3σ_Ẏ - Lateral Drift - M/Sec
g2 - Accelerometer Gain

FIGURE 15

APPENDIX A

ANALOG SIMULATION

SCALED EQUATIONS

(1) Lateral Translation

$$\ddot{\bar{Y}} = g\,\frac{\phi_m}{\ddot{Y}_m}\,\bar{\phi} - gY'_{1E}\,\frac{\eta_{1m}}{\ddot{Y}_m}\,\bar{\eta}_1 - gY'_{2E}\,\frac{\eta_{2m}}{\ddot{Y}_m}\,\bar{\eta}_2$$

$$+ \frac{F_s}{m}\,\frac{\beta_m}{\ddot{Y}_m}\,\bar{\beta} + \frac{Q}{m}\,F_o\,\frac{\alpha_m}{\ddot{Y}_m}\,\bar{\alpha}$$

(2) Pitch Rotation

$$\ddot{\bar{\phi}} = \frac{F-X}{I}\left(X_E Y'_{1E} - Y_{1E}\right)\frac{\eta_{1m}}{\ddot{\phi}_m}\,\bar{\eta}_1$$

$$+ \frac{F-X}{I}\left(X_E Y'_{2E} - Y_{2E}\right)\frac{\eta_{2m}}{\ddot{\phi}_m}\,\bar{\eta}_2$$

$$- \frac{F_s}{I}\,X_E\,\frac{\beta_m}{\ddot{\phi}_m}\,\bar{\beta} - \frac{QF_1}{I}\,\frac{\alpha_m}{\ddot{\phi}_m}\,\bar{\alpha}$$

(3) Engine Gimbal and Control Equations

$$\ddot{\bar{\beta}} = -\frac{m_1}{m_2}\,\frac{\dot{\beta}_m}{\ddot{\beta}_m}\,\dot{\bar{\beta}} - \frac{1}{m_2}\,\frac{\beta_m}{\ddot{\beta}_m}\,\bar{\beta}$$

$$+ \frac{a_o}{m_2}\,\frac{\phi_m}{\ddot{\beta}_m}\,\bar{\phi} - \frac{a_o}{m_2}\,Y'_{1g}\,\frac{\eta_{1m}}{\ddot{\beta}_m}\,\bar{\eta}_1$$

$$- \frac{a_o}{m_2}\,Y'_{2g}\,\frac{\eta_{2m}}{\ddot{\beta}_m}\,\bar{\eta}_2 + \frac{a_1}{m_2}\,\frac{\dot{\phi}_m}{\ddot{\beta}_m}\,\dot{\bar{\phi}}$$

$$- \frac{a_1}{m_2}\,Y'_{1g}\,\frac{\dot{\eta}_{1m}}{\ddot{\beta}_m}\,\dot{\bar{\eta}}_1 - \frac{a_1}{m_2}\,Y'_{2g}\,\frac{\dot{\eta}_{2m}}{\ddot{\beta}_m}\,\dot{\bar{\eta}}_2$$

$$- \frac{g_{21}}{m_2}\,\frac{A_{1m}}{\ddot{\beta}_m}\,\bar{A}_1 + \frac{g_3}{m_2}\,\frac{\dot{Y}_m}{\ddot{\beta}_m}\,\dot{\bar{Y}}$$

$$+ \frac{g_4}{m_2}\,\frac{\alpha_m}{\ddot{\beta}_m}\,\bar{\alpha}$$

(4) Lateral Acceleration

$$\bar{\ddot{A}}_1 = \left[\frac{\ddot{Y}_m}{\ddot{A}_{1m}} \bar{\ddot{Y}} - X_{A_1} \frac{\ddot{\phi}_m}{\ddot{A}_{1m}} \bar{\ddot{\phi}} - g \frac{\phi_m}{\ddot{A}_{1m}} \bar{\phi} + Y_{1_{A_1}} \frac{\ddot{\eta}_{1m}}{\ddot{A}_{1m}} \bar{\ddot{\eta}}_1 + Y_{2_{A_1}} \frac{\ddot{\eta}_{2m}}{\ddot{A}_{1m}} \bar{\ddot{\eta}}_2 + gY'_{1_{A_1}} \frac{\eta_{1m}}{\ddot{A}_{1m}} \bar{\eta}_1 + gY'_{2_{A_1}} \frac{\eta_{2m}}{\ddot{A}_{1m}} \bar{\eta}_2 \right] \omega^2_{a_1} - \frac{\omega^2_{A_1} A_{1m}}{\ddot{A}_{1m}} \bar{A}_1 - \frac{2\zeta_{A_1}\omega_{A_1}\dot{A}_{1m}}{\ddot{A}_{1m}} \bar{\dot{A}}_1$$

(5) Angle of Attack

$$\bar{\alpha} = \frac{\phi_m}{\alpha_m} \bar{\phi} - \frac{1}{V} \frac{\dot{Y}_m}{\alpha_m} \bar{\dot{Y}} + \frac{1}{V} \frac{V_{wm}}{\alpha_m} V_w$$

(6) Bending Moment

$$\bar{B}_{m_R} = M'_\alpha \frac{\alpha_m}{B_{mR_m}} \bar{\alpha} + M'_\beta \frac{\beta_m}{\beta_{mR_m}} \bar{\beta}$$

(7) First Bending Mode

$$\bar{\ddot{\eta}}_1 = - \frac{2\zeta_{B_1}\omega_{B_1}\dot{\eta}_{1m}}{\ddot{\eta}_{1m}} \bar{\dot{\eta}}_1 - \omega^2_{B_1} \frac{\eta_{1m}}{\ddot{\eta}_{1m}} \bar{\eta}_1 + \frac{QD_1}{M_{B_1}} \frac{\alpha_m}{\ddot{\eta}_{1m}} \bar{\alpha} + \frac{F_s Y_{1E}}{M_{B_1}} \frac{\beta_m}{\ddot{\eta}_{1m}} \bar{\beta}$$

(8) Mean Squared Lateral Drift

$$\bar{\sigma}_{\dot{Y}}^2 = \frac{3.14}{10} \int \frac{\dot{Y}_m^2}{\sigma^2_{\dot{Y}_m}} \int \bar{\dot{Y}}^2 \, dt$$

(9) Mean Squared Bending Mode

$$\bar{\sigma}^2_{BM} = \frac{3.14}{10} \int \frac{BM_m^2}{\sigma^2_{BM_m}} \int_0^\infty \overline{BM}_R^2 \, dt$$

(10) Weighting Filter Equation

$$\dot{\bar{V}}_w = - C_1 \left(\frac{V_{w_m}}{\dot{V}_{w_m}} \right) \bar{V}_w - C_2 \left(\frac{\overline{\int}_{max} V_w}{\dot{V}_{w_m}} \right) \overline{\int} V_w dt$$

$$+ C_3 \left(\frac{\overline{\int}_{max} V_w^*}{V_{w_m}} \right) \overline{\int} V^* dt + C_4 \left(\frac{V_m}{\dot{V}_{w_m}} \right) \bar{V}^*$$

MAXIMUM VALUES

$\ddot{Y}_m = 0.2\ m/sec^2$

$\dot{Y}_m = 0.5\ m/sec$

$Y_m = 20\ m$

$\ddot{\phi}_m = 0.01\ rad/sec^2$

$\dot{\phi}_m = 0.01\ rad/sec$

$\phi_m = 0.01\ rad$

$\ddot{\beta}_m = 8\ rad/sec^2$

$\dot{\beta}_m = 0.02\ rad/sec$

$\beta_m = 0.02\ rad$

$\ddot{A}_{1m} = 400\ m/sec^4$

$\dot{A}_{1m} = 10\ m/sec^3$

$A_{1m} = 1\ m/sec^2$

$\alpha_m = 0.2\ rad$

$V_{w_m} = 100\ m/sec$

$B_{R_m} = 200 \times 10^5$ Newtons-Meter

$\eta_{1m} = 0.1\ m$

$\dot{\eta}_{1m} = 0.4\ m/sec$

$\ddot{\eta}_m = 1.6\ m/sec^2$

$\dot{V}_{w_m} = 5.25\ m/sec^2$

$\int_{max} V_w = 190.\ m$

$\int_{max} V^* = 1.90$

$V^*_{w_m} = 1.0$

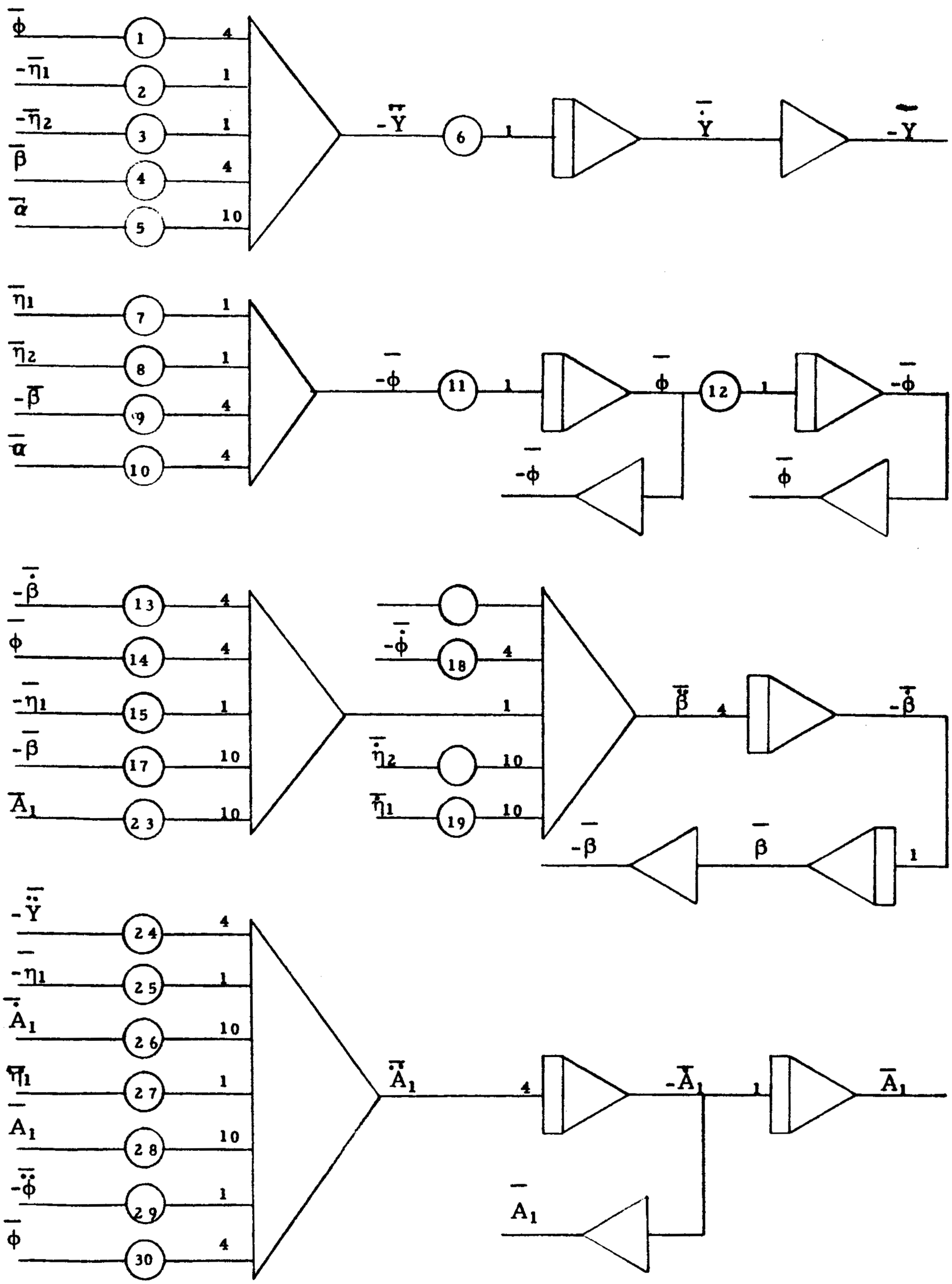

ANALOG DIAGRAM

FIGURE 16

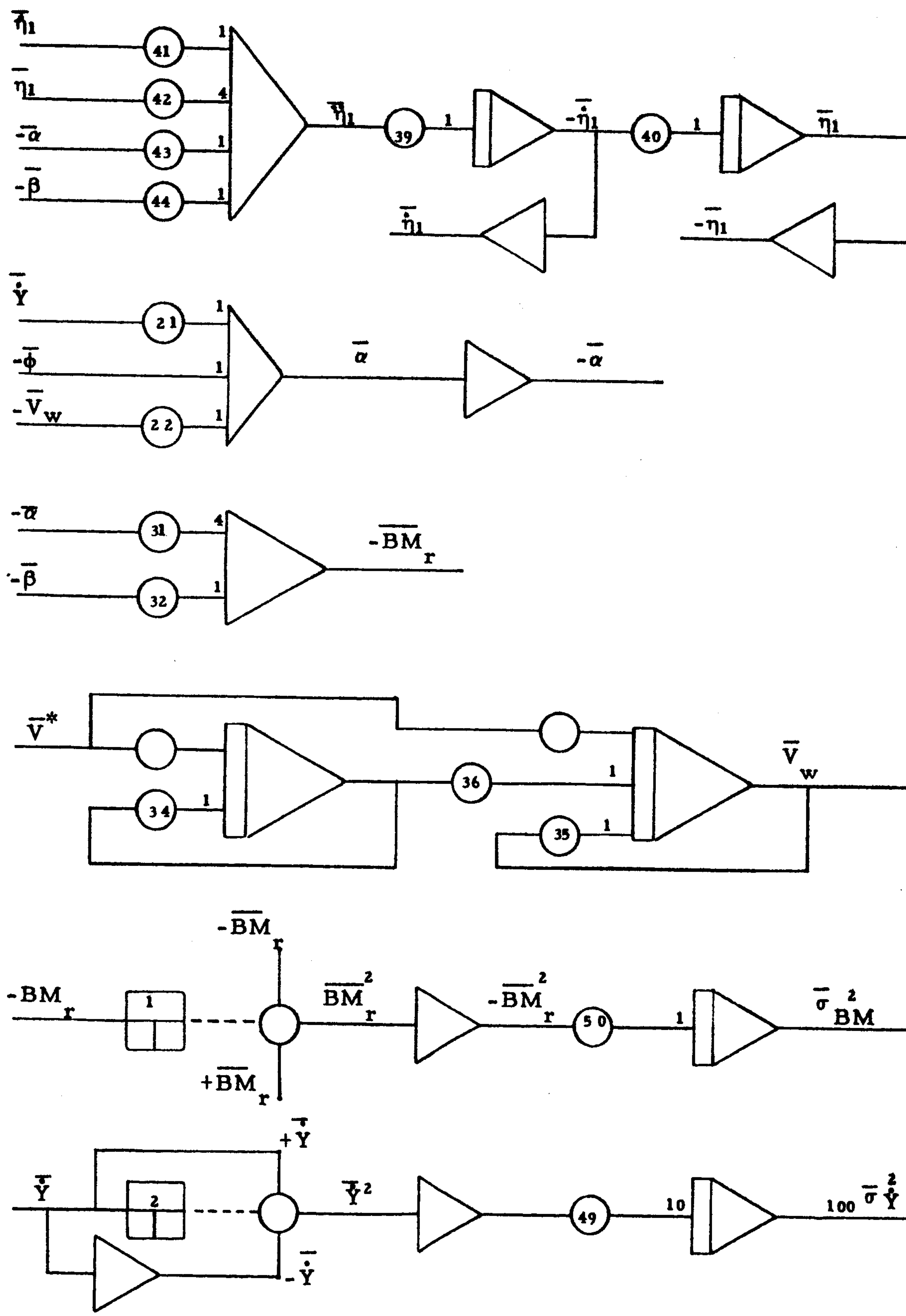

ANALOG DIAGRAM

FIGURE 16

CONTINUED

ANALOG DIAGRAM COMPONENT DEFINITIONS

POT NUMBERS	POT SETTINGS	POT DEFINITION	POT GAIN
(1)	0.264	$g(\phi_m / \ddot{Y}_m)$	4
(2)	0.532	$gY'_{1E}(\eta_{1m} / \ddot{Y}_m)$	1
(3)		$gY'_{2E}(\eta_{2m} / \ddot{Y}_m)$	
(4)	0.443	$\frac{F_s}{m}(\beta_m / \ddot{Y}_m)$	4
(5)	0.370	$\frac{QF_o}{m}(\alpha_m / \ddot{Y}_m)$	10
(6)	0.040	$\ddot{Y}_m / \dot{Y}_m$	10
(7)	0.244	$\frac{F-X}{I}(X_E Y'_{1E} - Y_{1E})\left(\frac{\eta_{1m}}{\ddot{\phi}_m}\right)$	1
(8)			
(9)	0.607	$\frac{F_s}{I} X_E (\beta_m / \ddot{\phi}_m)$	4
(10)	0.471	$\frac{QF_1}{I}(\alpha_m / \ddot{\phi}_m)$	4
(11)	0.100	$\ddot{\phi}_m / \dot{\phi}_m$	10
(12)	0.100	$\dot{\phi}_m / \phi_m$	10
(13)	0.292	$\frac{m_1}{m_2}(\dot{\beta}_m / \ddot{\beta}_m)$	4
(14)	0.160	$\frac{a_o}{m_2}(\phi_m / \ddot{\beta}_m)$	4

ANALOG DIAGRAM COMPONENT DEFINITIONS CONTINUED

POT NUMBERS	POT SETTINGS	POT DEFINITION	POT GAIN
(15)	0.242	$\frac{a_o}{m_2} Y'_{1g}\left(\frac{\eta_{1m}}{\ddot{\beta}_m}\right)$	1
(16)			
(17)	0.264	$\frac{1}{m_2}(\beta_m/\ddot{\beta}_m)$	10
(18)	0.358	$\frac{a_1}{m_2}(\dot{\phi}_m/\ddot{\beta}_m)$	4
(19)	0.222	$-\frac{a_1}{m_2}(Y_{1g}')(\ddot{\eta}_{1m}/\ddot{\beta}_m)$	10
(20)			
(21)	0.00475	$\frac{1}{V}\left(\frac{\dot{Y}_m}{\alpha_m}\right)$	1
(22)	0.929	$\frac{1}{V}\left(\frac{Y_{w_m}}{\alpha_m}\right)$	
(23)	0.514	$\frac{g_{21}}{m_2}(A_{1m}/\ddot{\beta}_m)$	10
(24)	.338	$\omega^2_{A_1}\ddot{Y}_m/\ddot{A}_{1m}$	4
(25)	.183	$\omega^2_{A_1} g Y'_{1A_1}(\eta_{1m}/\ddot{A}_{1m})$	4
(26)	.455	$\frac{2\zeta_{A_1}\omega_{A_1}\dot{A}_{1m}}{A_{1m}}$	4
(27)	.735	$\omega^2_{A_1} Y_{1A_1}(\ddot{\eta}_{1m}/\ddot{A}_{1m})$	4

ANALOG DIAGRAM COMPONENT DEFINITIONS CONTINUED

POT NUMBERS	POT SETTINGS	POT DEFINITION	POT GAIN
(28)	.626	$\omega^2_{A_1} \left(\frac{A_{1m}}{\ddot{A}_{1m}}\right)$	10
(29)	0	$\omega^2_{A_1} X_{A_1} (\ddot{\phi}_m / \ddot{A}_{1m})$	1
(30)	.356	$\omega^2_{A_1} X_{A_1} (\ddot{\phi}_m / \ddot{A}_{1m})$	4
(31)	0.288	$M'_\alpha (\alpha_m / BM_m)$	4
(32)	-0.304	$M'_\beta (\beta_m / BM_m)$	1
(33)			
(34)			
(35)			
(36)			
(37)			
(38)			
(39)	0.400	$\ddot{\eta}_{1m} / \dot{\eta}_{1m}$	1
(40)	0.400	$\dot{\eta}_{1m} / \eta_{1m}$	1

ANALOG DIAGRAM COMPONENT DEFINITIONS CONTINUED

POT NUMBERS	POT SETTINGS	POT DEFINITION	POT GAIN
(41)	0.0167	$\frac{2\zeta_{B_1} W_{B_1} \dot{\eta}_{1m}}{\ddot{\eta}_{1m}}$	1
(42)	0.700	$\omega^2_{B_1} (\eta_{1m}/\dot{\eta}_{1m})$	4
(43)	0.545	$\left(\frac{QD_1}{M_{B_1}}\right)\left(\frac{\alpha_m}{\ddot{\eta}_{1m}}\right)$	1
(44)	0.302	$\frac{F_s Y_{1E}}{M_{B_1}} \frac{\beta_m}{\ddot{\eta}_{1m}}$	1
(45)			
(46)			
(47)			
(48)			
(49)	0.0785	$3.14\ \dot{Y}^2_m/\sigma^2_{\dot{Y}_m}$	
(50)	0.314	$\left(\frac{3.14}{10}\right) \frac{BM^2_m}{\sigma^2_{BM_m}}$	

GEORGE C. MARSHALL SPACE FLIGHT CENTER
HUNTSVILLE, ALABAMA

Memorandum

TO NASA Scientific & Technical Information Facility, P. O. Box 33, College Park, Maryland 20740

DATE April 27, 1966

FROM R. L. Scott, MS-I

SUBJECT Contract NAS 8-20201; Reports and DRF's

Transmittal of:

1. Two (2) copies of LAUNCH VEHICLE WIND RESPONSE BY STATISTICAL METHODS, ER-1193, 29 November 1965
2. Document Release Form executed by Robert S. Ryan, R-AERO-DD, April 24, 1966 authorizing public announcement and distribution of the report in 1.
3. Two (2) copies of INVESTIGATION OF LATERAL ACCELERATION-BENDING COUPLING FOR A LARGE BOOSTER UTILIZING MULTI ACCELEROMETERS, ER-1213, 22 December 1965
4. Document Release Form by Robert S. Ryan, R-AERO-DD, April 24, 1966 authorizing announcement in STAR for report in 3.
5. Three (3) copies of SIMPLIFIED CRITERIA FOR MINIMUM LOAD AND DRIFT CONTROL OF LARGE BOOSTER VEHICLE, ER-1214, 22 December 1965
6. Document Release Form by Robert S. Ryan, R-AERO-DD, April 24, 1966 authorizing announcement of report in 5 in STAR.
7. Two (2) copies of INVESTIGATION OF NONLINEAR STRUCTURAL FEEDBACK IN BOOSTER CONTROL SYSTEMS, ER-1215, 22 December 1965
8. Document Release Form by Robert S. Ryan, R-AERO-DD, April 24, 1966 authorizing announcement of report in 7 in STAR.

All of the enclosed reports were prepared under contract NAS 8-20201 by Hayes International Corp., Birmingham, Alabama.

R. L. Scott
R. L. Scott

Enc as stated.